cated in Sf9 cells, it was not possible to determine the infectivity in the cases of the pseudotype baculoviruses possessing ligands incapable of entering into insect cells. To standardize the viral titer, we determined the amount of viral capsid protein vp39 by semiquantitative Western blot analysis. The infectious titer determined by plaque assay in Sf9 cells correlated well with the intensity of the vp39 signal obtained by Western blotting for both AcΔ64/gp64/CAluc and AcΔ64/VSVG/CAluc (data not shown). Pseudotype baculovirus titers are expressed as relative infectious units (RIU) in this study. To confirm the absence of gp64 in the bacmids, we synthesized oligonucleotide primers specific for the gp64 gene, the gp64 locus, and the vp39 gene as follows: for the gp64 gene, gp64-Fw (Bgl) (5′-AAAGATCTACCATGGTAAGCGCTATTGTTT-3′) and gp64-Rv (Sal) (5′-TTGTCGACTTAATATTGTCTATTACGGTTT-3′); for the gp64locus, gp64locus-Fw (5′-GCACGGATTGGGGAGAGGACGGATTTT-3′) and gp64locus-Rv (5′-AGCTCGTTATTCAAGTGTCCCGCGTAC-3′); and for vp39, vp39-Fw (5′-ATATGGCGCTAGTGCCCGTGGGTATGG-3′) and vp39-Rv (5′-GACGGCTATTCCTCCACCTGCTGCCTG-3′). PCR amplification was performed using *Taq* DNA polymerase (Invitrogen) according to the manufacturer's protocol.

Stability of pseudotype baculoviruses during passage in Sfgp64 cells. Culture supernatants from Sfgp64 cells transfected with recombinant bacmids were harvested 4 days after transfection. After serial passage in Sfgp64 cells for 4 days, each Sfgp64 cell supernatant was inoculated into Sf9 cells. The culture supernatants were further inoculated into Sf9 cells to examine the generation of replication-competent revertants during the replication in Sfgp64 cells. The presence of replication-competent virus in the culture supernatants was assessed by the appearance of cytopathic effect and GFP expression in Sf9 cells. GFP expression in insect cells was observed by fluorescence microscopy (UFX-II; Nikon, Tokyo, Japan). The generation of replication-competent viruses incorporating gp64 was examined by PCR using the viral DNA as a template. The supernatants of Sfgp64 cells were concentrated by centrifugation at 18,000 × *g* for 45 min at 4°C. Viral DNA, purified from replication-competent revertants by phenol-chloroform extraction, was examined by Southern blot analysis. DNA was digested with BglII or PstI, separated by electrophoresis on a 0.6% agarose gel, and transferred to a Hybond N+ nylon membrane (Amersham Biosciences, Piscataway, N.J.). PCR primers [gp64-Fw (Bgl) and gp64-Rv (Sal) for the gp64 gene or vp39-Fw and vp39-Rv for the vp39 gene] were used to amplify the target fragments for use as hybridization probes. PCR products were purified and labeled using the ECL direct nucleic acid labeling and detection system (Amersham Biosciences) according to the manufacturer's instructions. Fragments containing the gp64 or vp39 gene were visualized using image analyzer LAS-3000 (Fujifilm, Tokyo, Japan).

Incorporation of ligands into pseudotype particles. To examine the expression of ligand proteins in insect cells or the incorporation of the ligands into pseudotype particles, cell lysates or purified baculoviruses were separated by SDS-polyacrylamide gel electrophoresis and electroblotted onto Hybond-P polyvinylidene difluoride membranes (Amersham Bioscience). After being blocked in phosphate-buffered saline containing 5% skim milk and 0.05% Tween 20 (Sigma), the membranes were incubated at room temperature for 1 h with a rabbit polyclonal anti-CD46 antibody (H-294; 1:200) (Santa Cruz, Santa Cruz, Calif.) or one of the following mouse monoclonal antibodies: anti-gp64 (AcV5; 1:1,000) (kindly provided by P. Faulkner) (22), anti-VSVG (P5D4; 1:2,000) (Sigma), anti-SLAM (123317; 1:200) (R&D systems, Minneapolis, Minn.), or anti-vp39 (236; 1:2,000) (kindly provided by G. F. Rohrmann) (51). The membranes were then incubated in horseradish peroxidase-conjugated anti-mouse IgG or anti-rabbit IgG antibodies at room temperature for 1 h. Immunoreactive bands were visualized using enhanced-chemiluminescence Super Signal West Femto substrate (Pierce, Rockford, Ill.) (47).

Reporter gene expression by pseudotype baculoviruses. AcΔ64/gp64/CAluc and AcΔ64/VSVG/CAluc baculoviruses were inoculated into 3.0×10^4 293T and BHK cells. Twenty-four hours after infection, the cells were lysed in Bright-Glo luciferase substrate (Promega, Madison, Wis.) according to the manufacturer's instructions. Relative light units were measured using a luminometer (AB-2200; ATTO Co. Ltd., Tokyo, Japan). To demonstrate ligand-directed gene targeting by AcΔ64/CD46/CAluc, AcΔ64/SLAMCAluc, and AcΔ64/SLAMcyto7/CAluc baculoviruses, 3.0×10^4 BHK cells were cotransfected with either pCA-EdF and pCA-EdH or pCA-IcF and pCA-IcH and then infected with 5.0×10^6 RIU of pseudotype baculoviruses at 24 h posttransfection. Luciferase expression was determined after a 24-h incubation.

Inhibition of gene transduction by specific antibodies against ligands. To examine ligand-directed gene transduction by pseudotype baculoviruses, we examined the neutralization of gene transduction by antibodies specific for the ligands presented by the pseudotypes. The appropriate dilutions of anti-gp64 (AcV1), anti-VSVG (I1) (kindly provided by M. A. Whitt) (30), anti-CD46 (M75) (Seikagaku Co. Ltd., Tokyo, Japan), or anti-SLAM (IPO-3) (Biodesign International, Saco, Maine) antibodies were preincubated with each virus (10^6 RIU) at 37°C for 60 min and then inoculated into the appropriate target cells. After incubation at 37°C for 24 h, we determined the neutralization by the included antibodies from the reduction of luciferase expression.

Entry of pseudotype baculovirus into target cells. BHK cells expressing hemagglutinin and fusion proteins derived from the Edmonston strain of measles virus were preincubated with either ammonium chloride (2, 10, or 50 mM) (Wako Pure Chemical Industries, Osaka, Japan) or chloroquine (20, 100, or 500 μM) (Sigma) for 1 h. The cells were then inoculated with 1.0×10^6 RIU of AcΔ64/CD46/CAluc, AcΔ64/gp64/CAluc, or AcΔ64/VSVG/CAluc in the presence of the above-mentioned reagents. The effects of ammonium choloride and chloroquine on gene transduction by pseudotype baculoviruses were determined by the changes in luciferase expression.

Electron microscopy. Viral particles purified by ultracentrifugation as described above were put onto carbon-coated copper 400-mesh electron microscopy grids for 15 min. After being washed in water, the grids were negatively stained with 1% (wt/vol) uranyl acetate and examined using a Hitachi (Tokyo, Japan) H-7100 electron microscope at 75 kV. For immunoelectron microscopy, virus particles put onto grids were incubated with murine monoclonal antibodies specific for VSVG (I1) or CD46 (E4.3) (Santa Cruz) and then treated with a gold particle-conjugated anti-mouse IgG antibody (British Biocell International, Ltd., Cardiff, United Kingdom). Samples were stained and observed as described above.

RESULTS

Construction of recombinant AcMNPV lacking the gp64 gene. The gp64 gene of the AcMNPV bacmid, bMON14272, was replaced with the CAT gene by homologous recombination in Sf9 cells using a modification of the methods reported by Bideshi and Federici (5) and Lung et al. (33) (Fig. 1A). We cotransfected bMON14272 and a linearized p64locus/cat plasmid bearing the CAT gene in place of the gp64 gene into Sf9 cells. DNA, extracted from the cells 48 h after transfection, was then transformed into competent DH10B cells. The disruption of the gp64 gene in colonies selected with kanamycin and chloramphenicol was confirmed by PCR (data not shown). We also constructed a recombinant bacmid, bMONΔ64/GFP/CAluc, which contained the insertion of the GFP gene under the control of the polyhedrin promoter and the luciferase gene under the control of the CAG promoter into the polyhedrin locus of the gp64-null bacmid (Fig. 1B). Disruption of gp64 in bMONΔ64/GFP/CAluc was confirmed by PCR using a series of specific primers (Fig. 1C). PCR with primers specific for the vp39 gene, used as an internal control for the AcMNPV bacmid, amplified a 900-bp product from both the bMONΔ64/GFP/CAluc and parent bMON14272 bacmids. The gp64 gene (1,558 bp) was amplified from bMON14272 and pUC/64locus, but not from bMONΔ64/GFP/CAluc and p64locus/cat. The 2,741- and 2,143-bp fragments corresponding to the wild-type and mutant gp64 genes, respectively, were amplified using gp64 locus-specific primers. The wild-type gene was amplified from bMON14272 and pUC/gp64locus, while the mutant gene was amplified from bMONΔ64/GFP/CAluc and p64locus/cat (Fig. 1A and C). These data indicate that the gp64 gene was replaced with the cat gene in bMONΔ64/GFP/CAluc. Previous studies demonstrated that gp64-null AcMNPV could propagate in $Sf9^{OP64\text{-}6}$ or $Sf9^{Op1D}$ cell lines constitutively expressing the gp64 protein of *Orgyia pseudotsugata* NPV (OpNPV) but not in untransfected Sf9 cells (40, 49). We then established a cell line, Sfgp64, constitutively expressing the gp64 gene derived from AcMNPV. The pAFgp64 plasmid, carrying the gp64 gene of AcMNPV without any flanking sequence, was used to

avoid homologous recombination between the viral genome and the plasmid. To examine the replication competency of gp64-null AcMNPV (AcΔ64/GFP/CAluc), Sfgp64 and Sf9 cells were transfected with bMONΔ64/GFP/CAluc. We assessed the propagation of infectious virus by measuring GFP expression by fluorescence microscopy. Forty-eight hours posttransfection, ~10% of the Sfgp64 and Sf9 cells were GFP positive (data not shown). While Sfgp64 cells exhibited the spread of infection 96 h posttransfection, Sf9 cells did not (Fig. 1D). These data indicate that AcΔ64/GFP/CAluc can replicate only in Sfgp64 cells, not in Sf9 cells.

Appearance of revertants incorporating the gp64 gene during replication in Sfgp64 cells. To determine the stability of AcΔ64/GFP/CAluc during replication in Sfgp64 cells, we serially passaged AcΔ64/GFP/CAluc in Sfgp64 cells. Culture supernatants of Sfgp64 cells collected 4 days after transfection with bMONΔ64/GFP/CAluc (passage 1) were inoculated into Sfgp64 cells. The supernatants were further passaged in Sfgp64 cells for 4 days. To examine the appearance of replication-competent viruses, the culture supernatants from each passage were inoculated into Sf9 cells. At 4 days postinfection, we examined GFP expression in Sf9 cells by fluorescence microscopy (Fig. 2A). The expression of GFP was observed in Sf9 cells inoculated with Sfgp64 culture supernatants, irrespective of the passage history. As gp64-negative AcΔ64/GFP/CAluc baculovirus only transiently carries gp64, progeny viruses produced in Sf9 cells should not be infectious. The supernatants of Sf9 cells inoculated with supernatants recovered after >3 passages (passages 3, 4, and 5) with Sfgp64 cells exhibited infectivity to Sf9 cells, suggesting the generation of replication-competent revertants incorporating the gp64 gene into the viral genome. To confirm the incorporation of gp64 into the viral genome, virus particles were purified from the supernatants of each Sfgp64 passage. The presence of the gp64 gene within the viral genome was determined by PCR. We detected the gp64 gene in viruses obtained from the culture supernatants of passages 3, 4, and 5 but not in those from the first and second passages (Fig. 2B). Furthermore, PCR amplification of viral DNA with the gp64 locus-specific primers revealed that a 2,143-bp fragment, corresponding to the mutant form, was detected in the genome of AcΔ64/GFP/CAluc, while a 2,741-bp fragment, corresponding to the wild-type form, was amplified from Ac14272, irrespective of the number of passages. These results confirmed that the emergence of replication-competent virus during the passage in Sfgp64 cells is not due to the contamination of the parental virus, Ac14272. The recombinant virus incorporated the gp64 gene into the AcΔ64/GFP/CAluc genome during propagation in Sfgp64 cells.

Plasmid DNA can be integrated into multiple sites within the viral genome by nonhomologous recombination upon cotransfection of plasmid DNA with the baculovirus genome in Sf9 cells (71). To determine if gp64 genes integrated into the baculovirus genome by nonhomologous recombination during propagation in Sfgp64 cells, we analyzed the DNAs of three independent revertant viruses by PCR and Southern blot analyses. Viral DNA was extracted from these revertant viruses and analyzed by PCR as described above (Fig. 3A). We detected the gp64 gene in all revertant viruses and bMON14272 but not in the parental bacmid, bMONΔ64/GFP/CAluc. The gp64 locus primers amplified the mutant 2,143-bp fragment from all revertant viruses and the parental bMONΔ64/GFP/CAluc bacmid, not the 2,741-bp wild-type fragment that could be amplified from bMON14272. These results confirmed that the three independent revertant viruses, instead of deriving from contaminating wild-type virus, had incorporated the gp64 gene into their genomes exogenously. DNA from the revertants was digested with BglII or PstI, which do not digest sequences within the gp64 or vp39 genes, and hybridized to gp64- or vp39-specific probes (Fig. 3B). If the gp64 gene integrated into the viral genome by nonhomologous recombination, the digested fragments containing the gp64 gene would be of different sizes. Following digestion with BglII, the DNA fragments containing the gp64 gene in the revertants differed in size from each other (Fig. 3B, lanes 3 to 5). When digested with PstI, the sizes of the fragments containing the gp64 gene were similar in revertant clones 2 and 3 (Fig. 3B, lanes 9 to 10), indicating that the gp64 gene may have integrated into nearby sites in the viral genomes of clones 2 and 3. The fragment containing the gp64 gene in revertant clone 1 following digestion with either BglII or PstI was similar to that seen in bMON14272 (Fig. 3B lanes 3 and 8). These results, however, were not due to contamination with bMON14272, as the PCR analysis demonstrated that the gp64 locus of revertant clone 1 was of the mutant type (Fig. 3A). These data suggested that the gp64 gene integrated into the virus genomes of the revertants by nonhomologous recombination. As an internal control, the vp39 gene was detected in fragments of the predicted sizes (31,975 bp when digested with BglII and 29,009 bp when digested with PstI) in all viruses. To determine the sites of integration of the gp64 gene in the genomes of the revertants, we tried to sequence from within the gp64 gene out into the baculovirus genome by using an internal gp64 primer. In revertant 2, the sequences including the actin promoter and the gp64 gene were detected upstream of the polyhedrin promoter, where no homologous sequence was observed. In revertants 1 and 3, however, sequence analyses by the internal primer obtained only sequences of pAFgp64 and could not reach the integration site, due to a large insertion of the plasmid sequence (data not shown).

Characterization of pseudotype baculovirus carrying VSVG. Previous studies demonstrated that the gp64 protein plays a critical role in infection of various mammalian cells, as well as insect cells (66). To determine if the pseudotype baculoviruses bearing foreign viral envelope proteins in place of gp64 can infect and express foreign genes within mammalian cells, we constructed a gp64-null pseudotype virus, AcΔ64/VSVG/CAluc, by the transfection of bMONΔ64/VSVG/CAluc, which encodes the VSVG gene under the control of the polyhedrin promoter and the luciferase gene under the control of the CAG promoter, into Sf9 cells (Fig. 1B). As a control, we also generated AcΔ64/gp64/CAluc, in which the gp64 gene under the control of the polyhedrin promoter replaced the VSVG gene in the above-mentioned virus. Sf9 cells were transfected with appropriate bacmids and incubated for 4 days. The pseudotype baculoviruses in the culture supernatants were concentrated and purified by ultracentrifugation (10^8 to 10^9 RIU/ml). To examine the expression and incorporation of the glycoproteins into virions, we transfected these bacmid constructs into Sf9 cells. The cell lysates and the purified virus particles were examined by Western blot analysis (Fig. 4A). VSVG and gp64

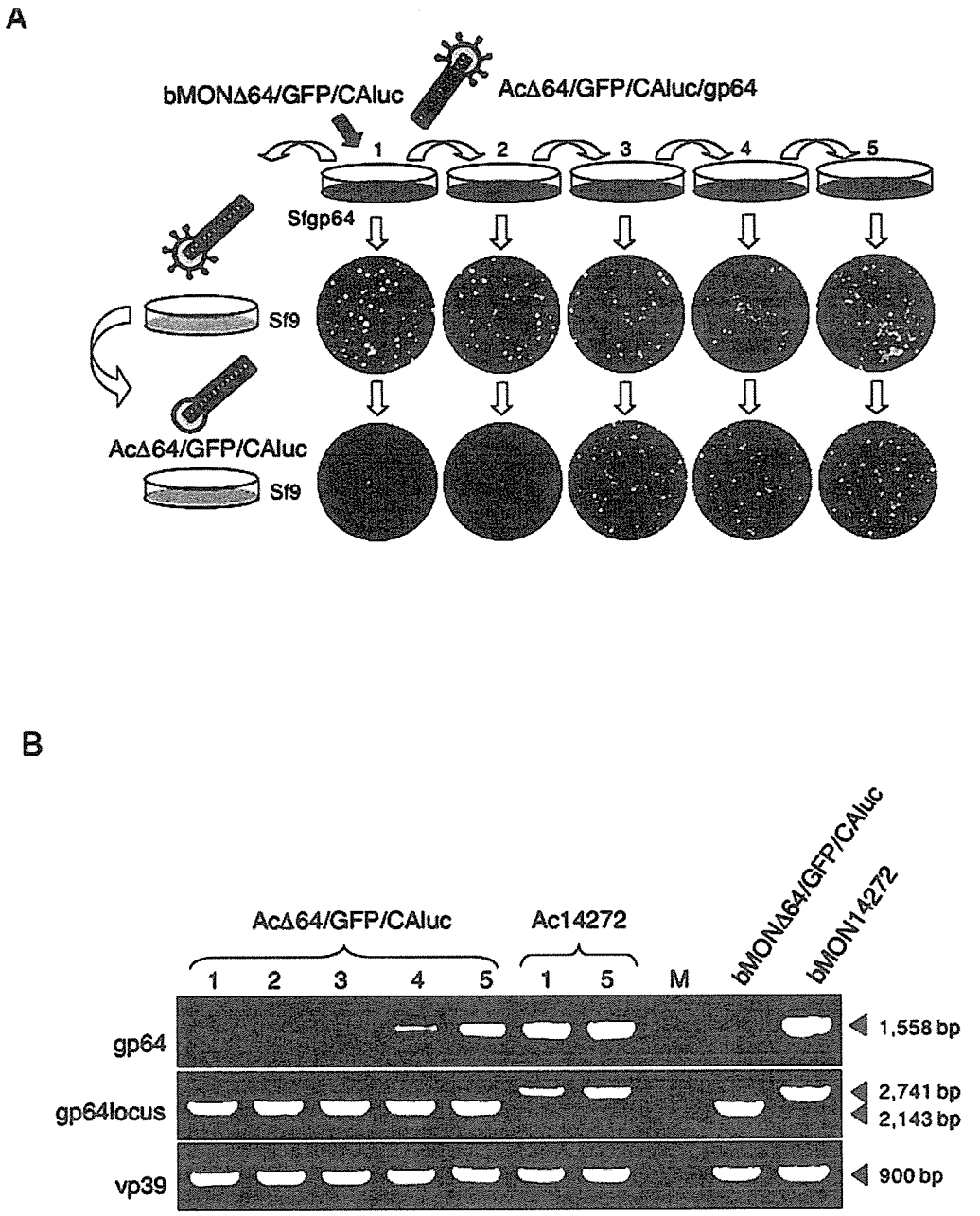

FIG. 2. Appearance of replication-competent viruses incorporating the gp64 gene during passage in Sfgp64 cells. (A) Sfgp64 cells were transfected with bMONΔ64/GFP/CAluc. Culture supernatants were harvested 4 days after transfection and then serially passaged in Sfgp64 cells at 4-day intervals. Each culture supernatant from Sfgp64 cells was passaged two more times in Sf9 cells to detect the appearance of replication-competent viruses. GFP expression in Sf9 cells was examined by fluorescence microscopy 4 days after infection. (B) PCR analysis of purified virus particles from the supernatant of each Sfgp64 cell passage. The gp64 gene was detectable in particles obtained from the third or later passages. The numbers above the lanes represent the passage numbers. The bMONΔ64/GFP/CAluc and bMON14272 bacmids and Ac14272, generated from bMON14272 and passaged in Sfgp64 cells, were used as controls. M is the culture supernatant of uninfected Sfgp64 cells concentrated under the same conditions as the virus particles. The primers amplified fragments as detailed in the legend to Fig. 1.

were expressed in the cells transfected with the appropriate bacmids. The proteins were also detected in the purified AcΔ64/VSVG/CAluc and AcΔ64/gp64/CAluc viruses, respectively, but not in AcΔ64/GFP/CAluc.

To assess the efficacy of mammalian cell gene transduction by the pseudotype baculoviruses, 293T and BHK cells were inoculated with various amounts of pseudotype viruses (Fig. 4B). Similar levels of reporter gene expression were observed in a dose-dependent manner in both cell lines following infection with AcΔ64/gp64/CAluc and AcΔ64/VSVG/CAluc. AcΔ64/GFP/CAluc, however, was unable to infect either cell line. To confirm the role of gp64- or VSVG-mediated gene transduction into mammalian cells by the pseudotype baculoviruses, we attempted to neutralize 293T cell infection using

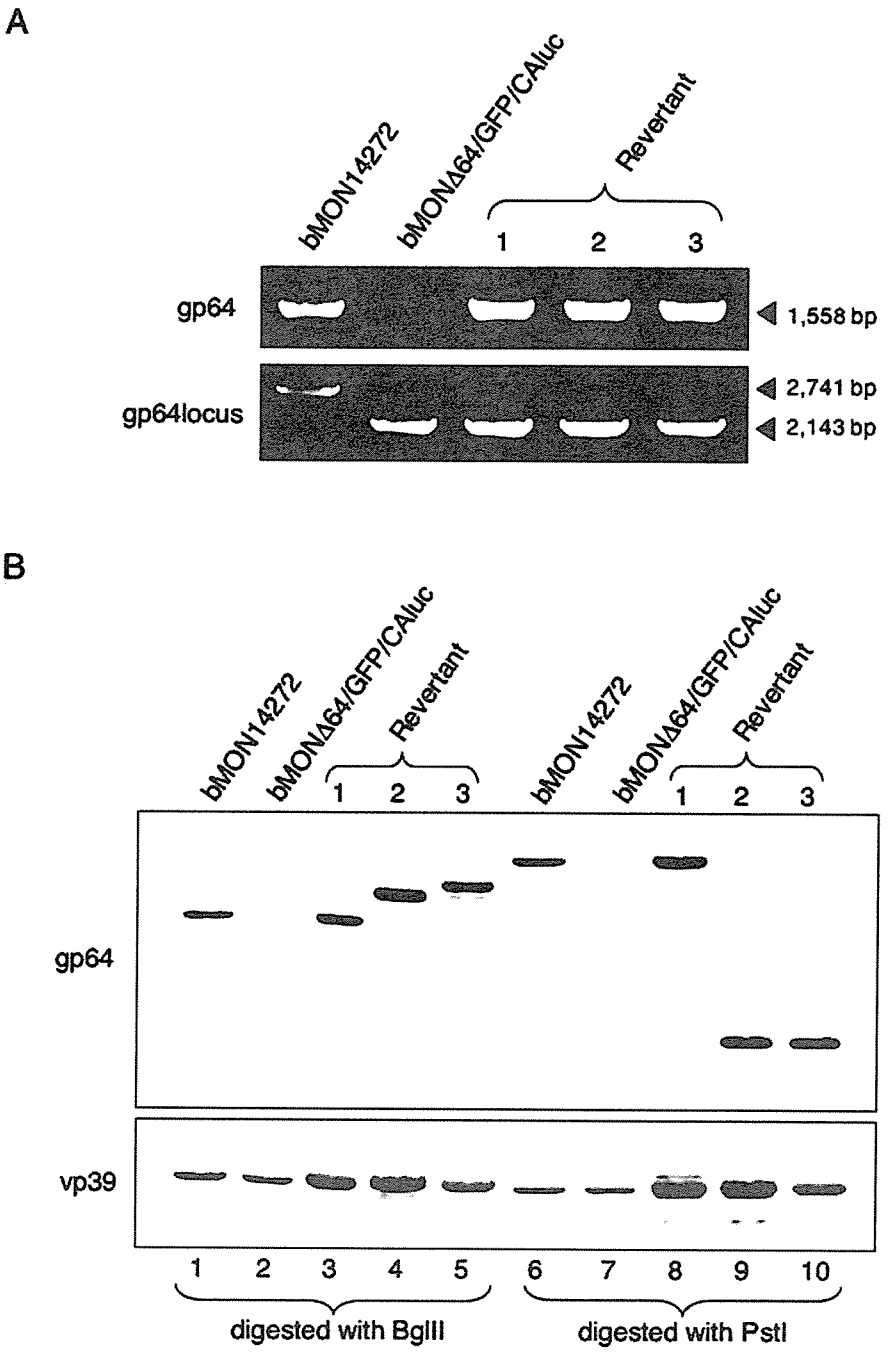

FIG. 3. Incorporation of the gp64 gene into gp64-null baculovirus genomes by nonhomologous recombination. (A) PCR analysis of three independent revertant viruses. In each revertant virus, the gp64 gene and gp64 locus primer pairs produced 1,558- and 2,143-bp fragments, respectively, indicating the presence of the mutant gp64 locus. (B) Southern blot analysis of revertant viruses. Viral DNA was digested with BglII or PstI, separated, and hybridized to gp64- or vp39-specific probes. Fragments containing the gp64 gene were detectable in all of the revertant viruses, but the fragment sizes differed. The vp39 gene, used as an internal control, was detectable in all revertant DNAs and bacmids. The numbers above the lanes represent the revertant clones. The bMONΔ64/GFP/CAluc and bMON14272 bacmids were used as controls.

specific monoclonal antibodies against gp64 and VSVG. Luciferase expression in 293T cells infected with either AcΔ64/gp64/CAluc or AcΔ64/VSVG/CAluc was specifically inhibited by antibodies against gp64 or VSVG, respectively (Fig. 4C). These results indicate that reporter gene expression in mammalian cells inoculated with pseudotype baculoviruses relies on the interactions mediated by the ligand proteins on the viral particles.

Ligand-directed gene targeting by pseudotype baculovirus. To demonstrate the ligand-directed gene transduction of target cells by pseudotype baculoviruses, we constructed pseudotype viruses bearing CD46 or SLAM in place of the gp64

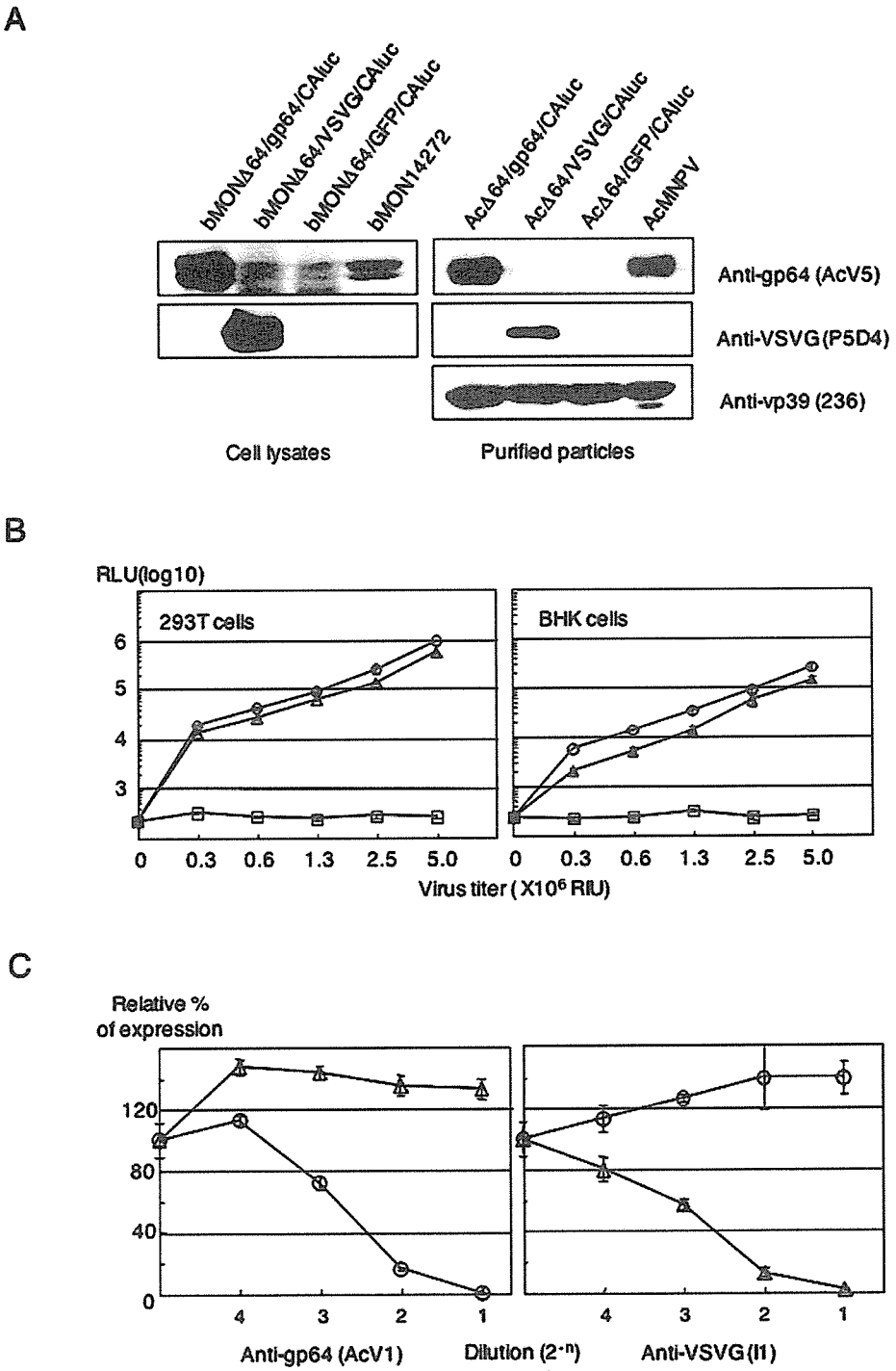

FIG. 4. Characterization of pseudotype baculoviruses bearing VSVG. (A) VSVG and gp64 expression in Sf9 cells transfected with the bMONΔ64/gp64/CAluc, bMONΔ64/VSVG/CAluc, bMONΔ64/GFP/CAluc, or bMON14272 bacmid were examined by Western blot analysis using monoclonal antibodies specific for VSVG (P5D4) and gp64 (AcV5) (left). The incorporation of gp64 and VSVG into pseudotype particles, AcΔ64/gp64/CAluc, AcΔ64/VSVG/CAluc, AcΔ64/GFP/CAluc, or AcMNPV, was examined by Western blot analysis using monoclonal antibodies specific for gp64, VSVG, and vp39 (236) (right). (B) Gene transduction into mammalian cells by pseudotype baculoviruses. 293T or BHK cells (3×10^4) were inoculated with various amounts of AcΔ64/gp64/CAluc, AcΔ64/VSVG/CAluc, or AcΔ64/GFP/CAluc. The pseudotype titers are expressed as RIU. Luciferase expression was determined 24 h after infection. The results shown are the means of three independent assays, while the error bars represent the standard deviations. RLU, relative light units. (C) Neutralization of gene transduction into mammalian cells by pseudotype baculoviruses by antibodies specific for the particle ligands. AcΔ64/gp64/CAluc or AcΔ64/VSVG/CAluc (10^6 RIU) was preincubated with the indicated dilutions of monoclonal antibodies specific for gp64 (AcV1) or VSVG (I1), respectively, for 60 min at 37°C. Residual activity, determined as luciferase expression in 293T cells 24 h postinfection, is expressed as the relative percentages of expression. The results shown are the means of three independent assays, with the error bars representing the standard deviations.

protein. The receptor usage of measles virus has been well characterized; while laboratory strains of measles virus, such as the Edmonston strain, can use either CD46 or SLAM as receptors, wild-type strains, such as the Ichinose strain, can only use SLAM for entry (15, 24, 42, 48, 67). Expression of these receptor molecules in Sf9 cells transfected with the bMONΔ64/CD46/CAluc or bMONΔ64/SLAM/CAluc bacmid (Fig. 1B) and subsequent incorporation of the receptors into progeny particles (AcΔ64/CD46/CAluc and AcΔ64/SLAM/CAluc, respectively) were confirmed by Western blotting (Fig. 5A). CD46 was detected in cells transfected with bMONΔ64/CD46/CAluc and in the purified particles of AcΔ64/CD46/CAluc, whereas SLAM was detected in cells transfected with the bacmid but not in the particles of AcΔ64/SLAM/CAluc.

The gp64, CD46, and SLAM proteins are all type I membrane proteins. SLAM has a 77-amino-acid cytoplasmic domain (23), while gp64 and CD46 have only 7- and 33-amino-acid tails, respectively (49, 60). Therefore, we speculated that SLAM may be only inefficiently incorporated into baculovirus particles, due to its large cytoplasmic domain. To examine the effect of the cytoplasmic domain length on incorporation into baculovirus particles, we constructed a mutant SLAM molecule, SLAMcyto7, with a deletion in the C-terminal cytoplasmic domain that preserves only the seven membrane-proximal amino acids. Western blot analysis revealed that SLAMcyto7 was efficiently expressed in Sf9 cells transfected with bMONΔ64/SLAMcyto7/CAluc and subsequently incorporated into AcΔ64/SLAMcyto7/CAluc particles at levels similar to those seen for CD46 inclusion into AcΔ64/CD46/CAluc (Fig. 5A).

To determine the efficiency of ligand-directed gene delivery, BHK cells were cotransfected with expression plasmids encoding the measles virus H and F glycoproteins of the Edmonston (EdH and EdF) or Ichinose (IcH and IcF) strain. These cells were inoculated with pseudotype baculoviruses (Fig. 5B). AcΔ64/CD46/CAluc exhibited gene delivery specifically to cells expressing EdH and EdF, but not IcH and IcF. Although the efficiency of gene transduction was 10 times lower than that seen with AcΔ64/CD46/CAluc, AcΔ64/SLAMcyto7/CAluc could also deliver a reporter gene to cells expressing the Edmonston and Ichinose strain glycoproteins but not to control cells. While AcΔ64/gp64/CAluc and AcΔ64/VSVG/CAluc could effectively deliver a reporter gene to all of the cells examined, AcΔ64/SLAM/CAluc was ineffective against all of the cell lines tested, likely due to the lack of SLAM incorporation into the virions.

To confirm ligand-directed gene delivery by AcΔ64/CD46/CAluc and AcΔ64/SLAMcyto7/CAluc to cells expressing appropriate measles virus glycoproteins, we tested the neutralization of gene transduction by specific monoclonal antibodies against CD46 and SLAM (Fig. 5C). Gene transduction of target cells by either AcΔ64/CD46/CAluc or AcΔ64/SLAMcyto7/CAluc, but not by AcΔ64/gp64/CAluc, could be inhibited in a dose-dependent manner by anti-CD46 and anti-SLAM monoclonal antibodies, respectively. These results indicate that pseudotype baculoviruses can deliver foreign genes to target cells in a ligand-directed manner.

Entry pathway of the pseudotype baculoviruses. Virus entry occurs either by the direct fusion of viral envelope proteins with the host plasma membrane at neutral pH, as seen for measles virus, or following receptor-mediated endocytosis, as seen for AcMNPV and VSV, in which envelope glycoproteins undergo conformational changes into a fusion-competent state, leading to fusion between viral and host membranes at low pH within endosomes (6, 36, 69). Ammonium chloride and chloroquine, which inhibit endosomal acidification, have been used as entry inhibitors for viruses that penetrate cells through receptor-mediated endocytosis (7). To examine the entry pathways used by the pseudotype baculoviruses, we examined the infectivity of AcΔ64/gp64/CAluc, AcΔ64/VSVG/CAluc, and AcΔ64/CD46/CAluc to BHK cells expressing EdH and EdF in the presence or absence of ammonium chloride or chloroquine (Fig. 6). Although these compounds inhibited gene transduction of BHK cells inoculated with AcΔ64/gp64/CAluc or AcΔ64/VSVG/CAluc in a dose-dependent manner, gene transduction by AcΔ64/CD46/CAluc was not inhibited. In contrast, ammonium chloride treatment enhanced gene expression following AcΔ64/CD46/CAluc infection. These results indicate that the pseudotype baculoviruses utilize entry pathways conferred by the nature of the ligand protein replacing gp64.

Morphology of pseudotype baculovirus. To address any alterations in pseudotype baculovirus morphology, we examined the AcMNPV, AcΔ64/VSVG/CAluc, and AcΔ64/CD46/CAluc virus particles by transmission electron microscopy (Fig. 7A to C). All of the pseudotype baculoviruses exhibited rod shapes and similar sizes, indistinguishable from the wild-type baculovirus. To examine the incorporation of exogenous ligands into the virion, purified AcΔ64/VSVG/CAluc and AcΔ64/CD46/CAluc particles were examined by immunoelectron microscopy using specific monoclonal antibodies against VSVG and CD46 (Fig. 7E and F). In both pseudotype viruses, gold particles were detected on the virion surface from the stalk to the head domains, indicating that VSVG and CD46 were incorporated into the AcΔ64/VSVG/CAluc and AcΔ64/CD46/CAluc virus particles, respectively.

DISCUSSION

Baculovirus is a useful tool for gene delivery to mammalian cells due to the large capacity of the virus to incorporate foreign genes, the wide host range, and the lack of replication in mammalian cells, providing minimal toxicity (29, 53, 55, 61, 68). The gp64 envelope glycoprotein, involved in attachment to both insect and mammalian cells, is required for low-pH-triggered membrane fusion following endocytosis during virus entry (6, 8, 12, 14, 20, 21, 31, 40, 41, 66, 69, 70). We have previously demonstrated that the interaction of gp64 with cell surface phospholipids may be important in baculovirus infection of mammalian cells (66). As the recombinant baculoviruses used for gene delivery to mammalian cells in this system retained the gp64 envelope glycoprotein, it was difficult to deliver foreign genes to specific target cells.

To generate a ligand-directed gene-targeting baculovirus vector, we established a bacmid system to produce recombinant baculoviruses in which the gp64 gene was replaced with other ligand genes of interest. The gp64 protein is required for efficient budding from Sf9 cells; the budding of a mutant virus lacking gp64 was reduced to 2% of that seen for wild-type baculovirus (49). Although AcΔ64/gp64/CAluc, a pseudotype virus in which gp64 was reintroduced into the gp64 deletion mutant, incorporated two to three times as much gp64 protein as seen in wild-type baculovirus (Fig. 4A), the infectious titers

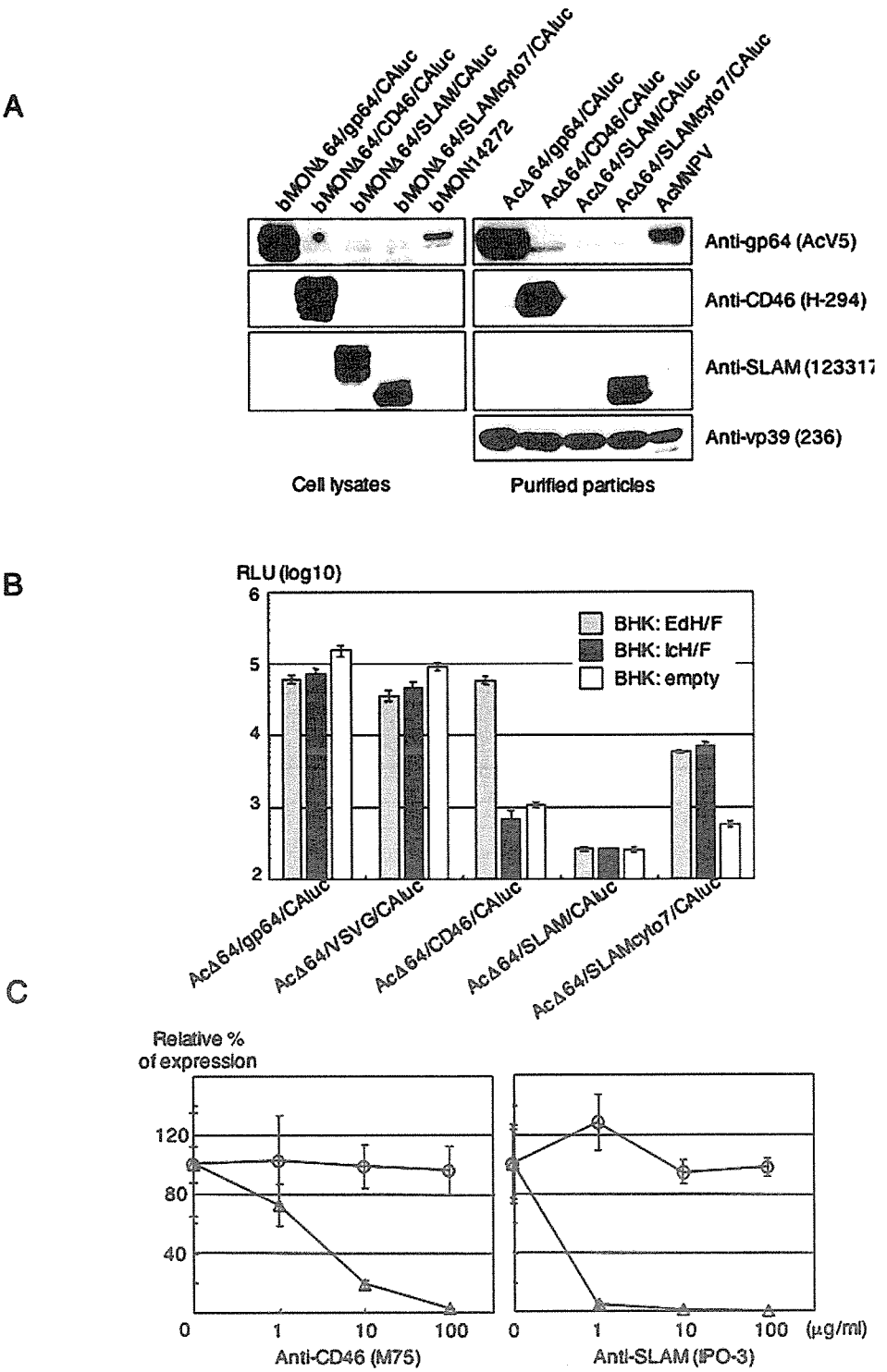

FIG. 5. Ligand-directed gene targeting by pseudotype baculoviruses. (A) The expression of gp64, CD46, SLAM, and SLAMcyto7 in Sf9 cells transfected with the bMONΔ64/gp64/CAluc, bMONΔ64/CD46/CAluc, bMONΔ64/SLAM/CAluc, bMONΔ64/SLAMcyto7/CAluc, or bMON14272 bacmid was examined by Western blot analysis using monoclonal antibodies specific for gp64 (AcV5), CD46 (H-294), and SLAM (123317), as indicated (left). The incorporation of gp64, CD46, SLAM, and SLAMcyto7 into pseudotype particles, AcΔ64/gp64/CAluc, AcΔ64/CD46/CAluc, AcΔ64/SLAM/CAluc, AcΔ64/SLAMcyto7/CAluc, or AcMNPV, was examined by Western blot analysis using monoclonal antibodies specific for gp64, CD46, SLAM, and vp39 (236), as indicated (right). (B) Ligand-directed gene targeting by pseudotype baculoviruses. BHK cells (3×10^4) were co-transfected with expression plasmids encoding measles virus H and F glycoproteins of either the Edmonston (EdH and EdF) or Ichinose (IcH and IcF) strain or with an empty vector and then inoculated with 5×10^6 RIU of AcΔ64/gp64/CAluc, AcΔ64/VSVG/CAluc, AcΔ64/CD46/CAluc, AcΔ64/SLAM/CAluc, or AcΔ64/SLAMcyto7/CAluc 24 h after transfection. Luciferase expression was determined 24 h after infection. The results shown are the means of three independent assays, and the error bars represent the standard deviations. RLU, relative light units. (C) Neutralization of ligand-directed gene targeting by antibodies specific for viral ligands. AcΔ64/gp64/CAluc, AcΔ64/CD46/CAluc, or AcΔ64/SLAMcyto7/CAluc (10^6 RIU) was preincubated with various concentrations of monoclonal antibodies specific for CD46 (M75) or SLAM (IPO-3) for 60 min at 37°C. Residual activity was determined by measurement of luciferase expression in BHK cells expressing the H and F glycoproteins of the Edmonston or Ichinose strain 24 h postinfection. The values are expressed as the relative percentages of expression. The results shown are the means of three independent assays, with the error bars representing the standard deviations.

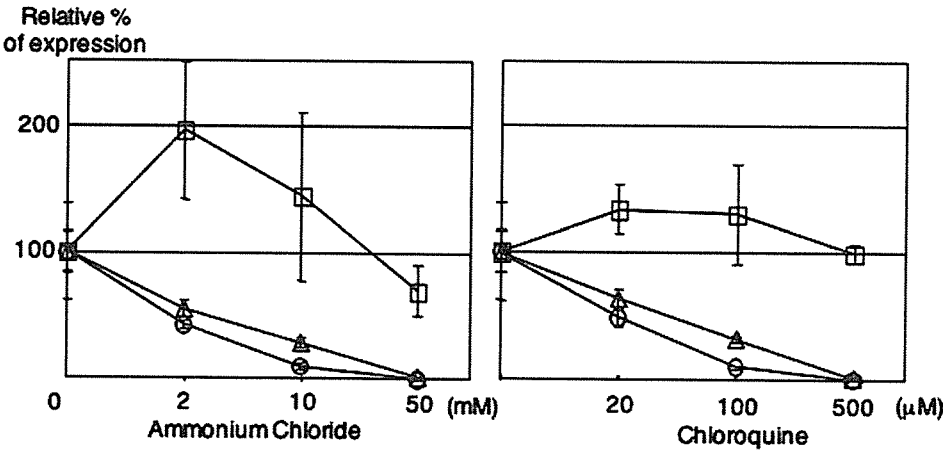

FIG. 6. Effects of lysosomotropic reagents on gene transduction of pseudotype baculoviruses. BHK cells (3×10^4) transfected with expression plasmids encoding the measles virus H and F glycoproteins of the Edmonston strain (EdH and EdF) were pretreated with various concentrations of ammonium chloride or chloroquine for 60 min. The cells were then inoculated with 10^6 RIU of AcΔ64/gp64/CAluc, AcΔ64/VSVG/CAluc, or AcΔ64/CD46/CAluc in the presence of the lysosomotropic reagents. Luciferase expression was determined 24 h postinfection. The results shown are the averages of three independent assays, with the error bars representing the standard deviations.

of the virus, determined by plaque formation in Sf9 cells, were similar. These results suggest that, while the polyhedrin promoter is sufficient to overexpress and incorporate a ligand of interest into the virion, this is not necessarily the best choice to maintain ligand function. The discrepancy between gp64 incorporation and the infectious titer may be attributed to a limited capacity to incorporate functional gp64 into particles and the timing of ligand gene activation. As the polyhedrin promoter is activated in the late stage of infection, baculoviruses budding in the early stage of infection may be unable to incorporate the ligand expressed by the polyhedrin promoter. Use of the immediate-early promoter for ligand expression may improve the efficiency of incorporation into virus particles. In support of this possibility, the infectious titer of a recombinant AcMNPV in which the gp64 gene was replaced with the F gene from *Lymantria dispar* NPV under the control of the polyhedrin promoter was ~60-fold lower than that of a virus with the F gene under the control of the gp64 promoter (33).

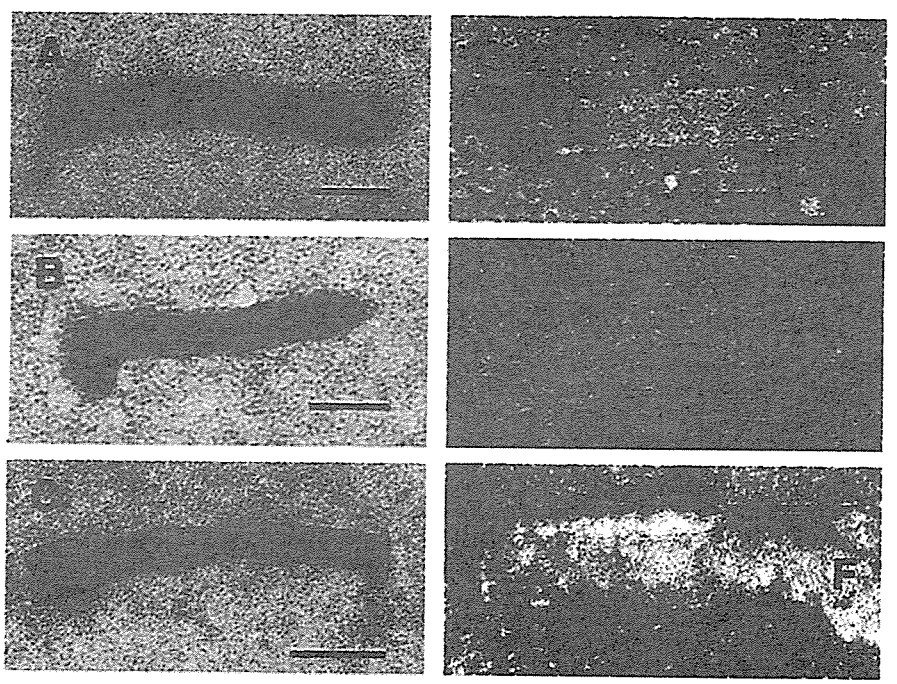

FIG. 7. Electron micrographs of pseudotype baculoviruses. Purified virus particles of wild-type AcMNPV (A), AcΔ64/VSVG/CAluc (B), and AcΔ64/CD46/CAluc (C) were examined by electron microscopy. A typical rod shape was visible in all of the pseudotype baculoviruses. The VSVG or CD46 proteins were observed on the surfaces of AcΔ64/VSVG/CAluc (E) and AcΔ64/CD46/CAluc (F) by immunoelectron microscopy using specific monoclonal antibodies against VSVG and CD46, respectively. AcMNPV treated with the monoclonal antibody against VSVG was used as a control (D). The bars on the panels represent 100 nm.

The replication competency in Sf9 cells of a gp64-null recombinant baculovirus could be rescued by incorporation of the VSVG gene (33, 34). We confirmed that the recombinant baculovirus deleted the gp64 gene and instead incorporated the VSVG gene under the control of the polyhedrin promoter, was replication competent in insect cells, and exhibited a high level of reporter gene transduction into 293T and BHK cells. The compatibility of VSVG in this system may result from similarities of the structural and functional characteristics of VSVG to those of gp64; both proteins are type I membrane glycoproteins, exist in trimeric complexes, and are capable of inducing membrane fusion at low pHs (6, 50, 54). Although the recombinant baculovirus in which gp64 is replaced with VSVG is able to replicate in insect cells and transduce foreign genes into a wide variety of mammalian cells, VSVG was suggested to recognize phosphatidylserine (58) or other ubiquitously expressed molecules other than phosphatidylserine (13) as a receptor(s), making it difficult to confer cell type specificity to gene delivery using VSVG pseudotype baculoviruses.

To establish ligand-directed gene delivery by pseudotype baculoviruses, it is necessary to propagate replication-deficient pseudotype baculoviruses possessing a ligand of interest in Sfgp64, a replication-competent cell line stably expressing gp64. After three rounds of passage of the pseudotype virus in Sfgp64 cells, however, replication-competent revertant viruses that had incorporated the gp64 gene were generated. Sfgp64 cells were established by transfection of Sf9 with a plasmid encoding the gp64 gene lacking any flanking sequences. Southern blot analysis revealed that the gp64 gene was integrated into the genomes of the baculovirus revertants by nonhomologous recombination. Homologous recombination between the AcMNPV genome and either a transfer vector (32, 38), additional AcMNPVs (19), or *B. mori* NPV can occur in insect cells with high frequency (27, 28). In contrast, our data suggest that the revertant viruses were not generated by homologous recombination but by nonhomologous incorporation of the gp64 gene from the Sfgp64 chromosome into the viral genome. Nonhomologous recombination between plasmid DNA and the baculovirus genome was previously reported upon cotransfection into insect cells (71). A gp64-null virus could propagate in $Sf9^{Op1D}$ cell lines constitutively expressing OpNPV gp64 without incorporating the gp64 gene into the viral genome (33, 34). One possible explanation for our result may be the difference between the gp64 genes of OpNPV and AcMNPV. Although the Sfgp64 cell line was established by sorting cells expressing a high level of gp64 on the cell surface, the expression level of gp64 might be lower than that of the $Sf9^{Op1D}$ cell line, and the lower level of expression of gp64 might result in the selective amplification of revertants. To circumvent the high-frequency incorporation of foreign DNA into the baculoviral genome, we attempted the lipofection of recombinant bacmids into Sf9 cells instead of amplification of pseudotype baculoviruses in Sfgp64. Although it is not possible to obtain a high pseudotype virus titer by this method, we can generate pure virus stocks without any contaminating replication-competent baculoviruses incorporating the gp64 gene. To prepare a high-titer stock of a replication-deficient pseudotype baculovirus carrying a foreign ligand, however, it is essential to propagate the pseudotype virus in Sf9 cells expressing gp64 without the transfection of plasmid DNA. Expression of gp64 by RNA transfection, RNA viral vectors, or the RNA replicon system may be able to avoid the incorporation of gp64 DNA into the baculovirus genome.

We constructed a pseudotype baculovirus, AcΔ64/CD46/CAluc, bearing human CD46 in place of gp64 on viral particles. CD46 is a multifunctional protein involved in the infection of various microorganisms and the regulation of complement activation (10). CD46, also known as membrane cofactor protein, protects autologous cells from complement attack by serving as a cofactor for factor I-mediated inactivation of C3b and C4b, blocking the complement cascade at C3 activation (2). CD46 also serves as a receptor for human herpes virus 6 (56), group B adenovirus (17, 59, 62), bovine viral diarrhea virus (39), two bacterial strains (*Streptococcus pyogenes* and pathogenic *Neisseria*) (26, 46), and the Edmonston strain of measles virus (15, 42). In this study, we demonstrated that AcΔ64/CD46/CAluc exhibited specific reporter gene transfer to and expression in BHK cells expressing the measles virus H and F glycoproteins of the Edmonston strain but not those expressing the Ichinose strain glycoproteins that require SLAM as a receptor (67). Therefore, a CD46 pseudotype baculovirus bearing a suicide gene may be able to eliminate cells expressing pathogen ligands that utilize CD46 as a receptor. Furthermore, CD46 is frequently overexpressed on cancer cells, possibly serving as a mechanism to overcome lysis by complement (16). In support of the potential utility of this vector, the Edmonston strain of measles virus has a potent and selective oncolytic activity (52). CD46 pseudotype baculovirus may also be applicable for the clearance of tumor cells surviving oncolytic measles virus treatment.

Infections with AcΔ64/gp64/CAluc and AcΔ64/VSVG/CAluc, carrying gp64 and VSVG on the particles, respectively, could be decreased by treatment with ATPase inhibitors, chloroquine, or ammonium chloride, while AcΔ64/CD46/CAluc was resistant to treatment. This finding suggests the possibility of constructing a baculovirus vector capable of both targeting and modulating the viral entry pathway, as seen for VSV (7). This is different from influenza virus vectors, where acidic exposure within endosomes is critical for the dissociation of the matrix protein from the ribonucleocapsid (9, 37). In contrast to AcΔ64/CD46/CAluc, AcΔ64/SLAM/CAluc could not incorporate the full-length SLAM molecule into particles, preventing specific gene transduction. The inability to mediate gene delivery was not due to the absence of an interaction with specific targets, as Sf9 cells expressing SLAM induced membrane fusion with BHK cells expressing the H and F glycoproteins of either the Edmonston or Ichinose strain of measles virus (data not shown). The ligands incorporated efficiently into baculovirus particles, including gp64, VSVG, and CD46, all have relatively short cytoplasmic domains, measuring 7, 29, and 33 amino acids in length, respectively (49, 54, 60). In contrast, SLAM possesses a cytoplasmic tail of 77 amino acids (23). We therefore hypothesized that the length of the ligand cytoplasmic domain may be critical for efficient incorporation into baculovirus particles. AcΔ64/SLAMcyto7/CAluc, possessing a mutant SLAM molecule with the C-terminal 70 amino acids of the cytoplasmic domain deleted, efficiently incorporated the mutant SLAM into particles and exhibited specific gene delivery to BHK cells expressing the H and F glycoproteins of both measles virus strains. Although the mechanism by which SLAM

incorporation into baculovirus particles is enhanced by C-terminal truncation of the cytoplasmic domain is not known, one possibility might be a change in SLAM localization. The gp64 protein localizes to the cell surface but is excluded from lipid raft microdomains (72). As VSVG and CD46 also do not associate with lipid rafts (35, 57), proteins localized to lipid raft microdomains may be excluded during virus assembly and budding. Although the cellular localization of SLAM is not known, further studies will be necessary to clarify the relationship between cell surface localization and incorporation into baculovirus particles and to test the involvement of lipid raft microdomains in this process.

Mangor et al. demonstrated that gp64-null baculoviruses pseudotyped with VSVG were not morphologically distinguishable from budded wild-type AcMNPV particles (34). We confirmed that AcΔ64/VSVG/CAluc, as well as AcΔ64/CD46/CAluc and AcΔ64/GFP/CAluc, exhibited a morphology similar to that of AcMNPV. These results indicate that expression of gp64 is not required for the morphogenesis of a rod-shaped structure for budded AcMNPV particles. Immunogold labeling of AcΔ64/VSVG/CAluc and AcΔ64/CD46/CAluc revealed that the VSVG and CD46 proteins were incorporated into and distributed throughout the whole viral surface. These results are consistent with previous observations that VSVG fusion proteins were distributed throughout the stalk and head domains of baculovirus particles, in contrast to gp64, which was primarily localized in the head domain (11, 44).

In this study, we have demonstrated the capability for ligand-directed gene delivery by pseudotype baculoviruses in vitro. For future in vivo applications of baculovirus vectors for gene targeting to specific organs or virus-infected cells as a method of treatment of inherited or infectious diseases, it is imperative to exhaustively study the transcription of baculoviral genes in mammalian cells for certification of safety. In addition, further studies are needed to establish replication-competent cell lines capable of supporting the propagation of pseudotype viruses without the possibility of replication-competent virus breakthrough by incorporation of gp64 and to optimize the conditions necessary for the efficient incorporation of ligands into recombinant baculovirus particles.

ACKNOWLEDGMENTS

We thank T. Seya and Y. Yanagi for kindly providing CHO cell lines; P. Faulkner, G. F. Rohrmann, and M. A. Whitt for their generous donation of antibodies; and H. Bando and K. Takeuchi for providing plasmids. We also thank H. Murase and I. Yanase for secretarial work and S. Ogawa for technical assistance.

This work was supported by grants-in-aid from the Ministry of Health, Labor, and Welfare in Japan and the 21st Century Center of Excellence Program of Japan.

REFERENCES

1. **Abe, T., H. Takahashi, H. Hamazaki, N. Miyano-Kurosaki, Y. Matsuura, and H. Takaku.** 2003. Baculovirus induces an innate immune response and confers protection from lethal influenza virus infection in mice. J. Immunol. **171:**1133–1139.
2. **Adams, E. M., M. C. Brown, M. Nunge, M. Krych, and J. P. Atkinson.** 1991. Contribution of the repeating domains of membrane cofactor protein (CD46) of the complement system to ligand binding and cofactor activity. J. Immunol. **147:**3005–3011.
3. **Ayres, M. D., S. C. Howard, J. Kuzio, M. Lopez-Ferber, and R. D. Possee.** 1994. The complete DNA sequence of *Autographa californica* nuclear polyhedrosis virus. Virology **202:**586–605.
4. **Barsoum, J., R. Brown, M. McKee, and F. M. Boyce.** 1997. Efficient transduction of mammalian cells by a recombinant baculovirus having the vesicular stomatitis virus G glycoprotein. Hum. Gene Ther. **8:**2011–2018.
5. **Bideshi, D. K., and B. A. Federici.** 2000. The *Trichoplusia ni* granulovirus helicase is unable to support replication of *Autographa californica* multicapsid nucleopolyhedrovirus in cells and larvae of *T. ni*. J. Gen. Virol. **81:**1593–1599.
6. **Blissard, G. W., and J. R. Wenz.** 1992. Baculovirus gp64 envelope glycoprotein is sufficient to mediate pH-dependent membrane fusion. J. Virol. **66:**6829–6835.
7. **Boritz, E., J. Gerlach, J. E. Johnson, and J. K. Rose.** 1999. Replication-competent rhabdoviruses with human immunodeficiency virus type 1 coats and green fluorescent protein: entry by a pH-independent pathway. J. Virol. **73:**6937–6945.
8. **Boyce, F. M., and N. L. Bucher.** 1996. Baculovirus-mediated gene transfer into mammalian cells. Proc. Natl. Acad. Sci. USA **93:**2348–2352.
9. **Bui, M., G. Whittaker, and A. Helenius.** 1996. Effect of M1 protein and low pH on nuclear transport of influenza virus ribonucleoproteins. J. Virol. **70:**8391–8401.
10. **Cattaneo, R.** 2004. Four viruses, two bacteria, and one receptor: membrane cofactor protein (CD46) as pathogens' magnet. J. Virol. **78:**4385–4388.
11. **Chapple, S. D., and I. M. Jones.** 2002. Non-polar distribution of green fluorescent protein on the surface of *Autographa californica* nucleopolyhedrovirus using a heterologous membrane anchor. J. Biotechnol. **95:**269–275.
12. **Chernomordik, L., E. Leikina, M. S. Cho, and J. Zimmerberg.** 1995. Control of baculovirus gp64-induced syncytium formation by membrane lipid composition. J. Virol. **69:**3049–3058.
13. **Coil, D. A., and A. D. Miller.** 2004. Phosphatidylserine is not the cell surface receptor for vesicular stomatitis virus. J. Virol. **78:**10920–10926.
14. **Condreay, J. P., S. M. Witherspoon, W. C. Clay, and T. A. Kost.** 1999. Transient and stable gene expression in mammalian cells transduced with a recombinant baculovirus vector. Proc. Natl. Acad. Sci. USA **96:**127–132.
15. **Dörig, R. E., A. Marcil, A. Chopra, and C. D. Richardson.** 1993. The human CD46 molecule is a receptor for measles virus (Edmonston strain). Cell **75:**295–305.
16. **Fishelson, Z., N. Donin, S. Zell, S. Schultz, and M. Kirschfink.** 2003. Obstacles to cancer immunotherapy: expression of membrane complement regulatory proteins (mCRPs) in tumors. Mol. Immunol. **40:**109–123.
17. **Gaggar, A., D. M. Shayakhmetov, and A. Lieber.** 2003. CD46 is a cellular receptor for group B adenoviruses. Nat. Med. **9:**1408–1412.
18. **Gronowski, A. M., D. M. Hilbert, K. C. Sheehan, G. Garotta, and R. D. Schreiber.** 1999. Baculovirus stimulates antiviral effects in mammalian cells. J. Virol. **73:**9944–9951.
19. **Hajós, J. P., J. Pijnenburg, M. Usmany, D. Zuidema, P. Závodszky, and J. M. Vlak.** 2000. High frequency recombination between homologous baculoviruses in cell culture. Arch. Virol. **145:**159–164.
20. **Hefferon, K., A. Oomens, S. Monsma, C. Finnerty, and G. W. Blissard.** 1999. Host cell receptor binding by baculovirus GP64 and kinetics of virion entry. Virology **258:**455–468.
21. **Hofmann, C., V. Sandig, G. Jennings, M. Rudolph, P. Schlag, and M. Strauss.** 1995. Efficient gene transfer into human hepatocytes by baculovirus vectors. Proc. Natl. Acad. Sci. USA **92:**10099–10103.
22. **Hohmann, A. W., and P. Faulkner.** 1983. Monoclonal antibodies to baculovirus structural proteins: determination of specificities by Western blot analysis. Virology **125:**432–444.
23. **Howie, D., M. Simarro, J. Sayos, M. Guirado, J. Sancho, and C. Terhorst.** 2002. Molecular dissection of the signaling and costimulatory functions of CD150 (SLAM): CD150/SAP binding and CD150-mediated costimulation. Blood **99:**957–965.
24. **Hsu, E. C., C. Iorio, F. Sarangi, A. A. Khine, and C. D. Richardson.** 2001. CDw150 (SLAM) is a receptor for a lymphotropic strain of measles virus and may account for the immunosuppressive properties of this virus. Virology **279:**9–21.
25. **Iwata, K., T. Seya, Y. Yanagi, J. M. Pesando, P. M. Johnson, M. Okabe, S. Ueda, H. Ariga, and S. Nagasawa.** 1995. Diversity of sites for measles virus binding and for inactivation of complement C3b and C4b on membrane cofactor protein CD46. J. Biol. Chem. **270:**15148–15152.
26. **Källström, H., M. K. Liszewski, J. P. Atkinson, and A. B. Jonsson.** 1997. Membrane cofactor protein (MCP or CD46) is a cellular pilus receptor for pathogenic *Neisseria*. Mol. Microbiol. **25:**639–647.
27. **Kamita, S. G., S. Maeda, and B. D. Hammock.** 2003. High-frequency homologous recombination between baculoviruses involves DNA replication. J. Virol. **77:**13053–13061.
28. **Kondo, A., and S. Maeda.** 1991. Host range expansion by recombination of the baculoviruses *Bombyx mori* nuclear polyhedrosis virus and *Autographa californica* nuclear polyhedrosis virus. J. Virol. **65:**3625–3632.
29. **Kost, T. A., and J. P. Condreay.** 2002. Recombinant baculoviruses as mammalian cell gene-delivery vectors. Trends Biotechnol. **20:**173–180.
30. **Lefrancois, L., and D. S. Lyles.** 1982. The interaction of antibody with the major surface glycoprotein of vesicular stomatitis virus. II. Monoclonal antibodies of nonneutralizing and cross-reactive epitopes of Indiana and New Jersey serotypes. Virology **121:**168–174.
31. **Leikina, E., H. O. Onaran, and J. Zimmerberg.** 1992. Acidic pH induces

fusion of cells infected with baculovirus to form syncytia. FEBS Lett. **304:** 221–224.
32. **Luckow, V. A., and M. D. Summers.** 1988. Trends in the development of baculovirus expression vectors. Biotechnology **6:**47–55.
33. **Lung, O., M. Westenberg, J. M. Vlak, D. Zuidema, and G. W. Blissard.** 2002. Pseudotyping *Autographa californica* multicapsid nucleopolyhedrovirus (Ac*M*NPV): F proteins from group II NPVs are functionally analogous to Ac*M*NPV GP64. J. Virol. **76:**5729–5736.
34. **Mangor, J. T., S. A. Monsma, M. C. Johnson, and G. W. Blissard.** 2001. A GP64-null baculovirus pseudotyped with vesicular stomatitis virus G protein. J. Virol. **75:**2544–2556.
35. **Manié, S. N., S. Debreyne, S. Vincent, and D. Gerlier.** 2000. Measles virus structural components are enriched into lipid raft microdomains: a potential cellular location for virus assembly. J. Virol. **74:**305–311.
36. **Marsh, M.** 1984. The entry of enveloped viruses into cells by endocytosis. Biochem. J. **218:**1–10.
37. **Martin, K., and A. Helenius.** 1991. Nuclear transport of influenza virus ribonucleoproteins: the viral matrix protein (M1) promotes export and inhibits import. Cell **67:**117–130.
38. **Matsuura, Y., R. D. Possee, H. A. Overton, and D. H. Bishop.** 1987. Baculovirus expression vectors: the requirements for high level expression of proteins, including glycoproteins. J. Gen. Virol. **68:**1233–1250.
39. **Maurer, K., T. Krey, V. Moennig, H. J. Thiel, and T. Rümenapf.** 2004. CD46 is a cellular receptor for bovine viral diarrhea virus. J. Virol. **78:**1792–1799.
40. **Monsma, S. A., A. G. Oomens, and G. W. Blissard.** 1996. The GP64 envelope fusion protein is an essential baculovirus protein required for cell-to-cell transmission of infection. J. Virol. **70:**4607–4616.
41. **Monsma, S. A., and G. W. Blissard.** 1995. Identification of a membrane fusion domain and an oligomerization domain in the baculovirus GP64 envelope fusion protein. J. Virol. **69:**2583–2595.
42. **Naniche, D., G. Varior-Krishnan, F. Cervoni, T. F. Wild, B. Rossi, C. Rabourdin-Combe, and D. Gerlier.** 1993. Human membrane cofactor protein (CD46) acts as a cellular receptor for measles virus. J. Virol. **67:**6025–6032.
43. **Niwa, H., K. Yamamura, and J. Miyazaki.** 1991. Efficient selection for high-expression transfectants with a novel eukaryotic vector. Gene **108:**193–199.
44. **Ojala, K., J. Koski, W. Ernst, R. Grabherr, I. Jones, and C. Oker-Blom.** 2004. Improved display of synthetic IgG-binding domains on the baculovirus surface. Technol. Cancer Res. Treat. **3:**77–84.
45. **Ojala, K., D. G. Mottershead, A. Suokko, and C. Oker-Blom.** 2001. Specific binding of baculoviruses displaying gp64 fusion proteins to mammalian cells. Biochem. Biophys. Res. Commun. **284:**777–784.
46. **Okada, N., M. K. Liszewski, J. P. Atkinson, and M. Caparon.** 1995. Membrane cofactor protein (CD46) is a keratinocyte receptor for the M protein of the group A streptococcus. Proc. Natl. Acad. Sci. USA **92:**2489–2493.
47. **Okamoto, K., K. Moriishi, T. Miyamura, and Y. Matsuura.** 2004. Intramembrane proteolysis and endoplasmic reticulum retention of hepatitis C virus core protein. J. Virol. **78:**6370–6380.
48. **Ono, N., H. Tatsuo, Y. Hidaka, T. Aoki, H. Minagawa, and Y. Yanagi.** 2001. Measles viruses on throat swabs from measles patients use signaling lymphocytic activation molecule (CDw150) but not CD46 as a cellular receptor. J. Virol. **75:**4399–4401.
49. **Oomens, A. G., and G. W. Blissard.** 1999. Requirement for GP64 to drive efficient budding of *Autographa californica* multicapsid nucleopolyhedrovirus. Virology **254:**297–314.
50. **Oomens, A. G., S. A. Monsma, and G. W. Blissard.** 1995. The baculovirus GP64 envelope fusion protein: synthesis, oligomerization, and processing. Virology **209:**592–603.
51. **Pearson, M. N., R. L. Russell, G. F. Rohrmann, and G. S. Beaudreau.** 1988. p39, a major baculovirus structural protein: immunocytochemical characterization and genetic location. Virology **167:**407–413.
52. **Peng, K. W., C. J. TenEyck, E. Galanis, K. R. Kalli, L. C. Hartmann, and S. J. Russell.** 2002. Intraperitoneal therapy of ovarian cancer using an engineered measles virus. Cancer Res. **62:**4656–4662.
53. **Pieroni, L., and N. La Monica.** 2001. Towards the use of baculovirus as a gene therapy vector. Curr. Opin. Mol. Ther. **3:**464–467.
54. **Rose, J. K., and M. A. Whitt.** 2001. Rhabdoviruses, p. 1221–1244. *In* D. M. Knipe and P. M. Howley (ed.), Fields virology, 4th ed. Lippincott Williams and Wilkins, Philadelphia, Pa.
55. **Sandig, V., and M. Strauss.** 1996. Liver-directed gene transfer and application to therapy. J. Mol. Med. **74:**205–212.
56. **Santoro, F., P. E. Kennedy, G. Locatelli, M. S. Malnati, E. A. Berger, and P. Lusso.** 1999. CD46 is a cellular receptor for human herpesvirus 6. Cell **99:** 817–827.
57. **Scheiffele, P., A. Rietveld, T. Wilk, and K. Simons.** 1999. Influenza viruses select ordered lipid domains during budding from the plasma membrane. J. Biol. Chem. **274:**2038–2044.
58. **Schlegel, R., T. S. Tralka, M. C. Willingham, and I. Pastan.** 1983. Inhibition of VSV binding and infectivity by phosphatidylserine: is phosphatidylserine a VSV-binding site? Cell **32:**639–646.
59. **Segerman, A., J. P. Atkinson, M. Marttila, V. Dennerquist, G. Wadell, and N. Arnberg.** 2003. Adenovirus type 11 uses CD46 as a cellular receptor. J. Virol. **77:**9183–9191.
60. **Seya, T., A. Hirano, M. Matsumoto, M. Nomura, and S. Ueda.** 1999. Human membrane cofactor protein (MCP, CD46): multiple isoforms and functions. Int. J. Biochem. Cell Biol. **31:**1255–1260.
61. **Shoji, I., H. Aizaki, H. Tani, K. Ishii, T. Chiba, I. Saito, T. Miyamura, and Y. Matsuura.** 1997. Efficient gene transfer into various mammalian cells, including non-hepatic cells, by baculovirus vectors. J. Gen. Virol. **78:**2657–2664.
62. **Sirena, D., B. Lilienfeld, M. Eisenhut, S. Kälin, K. Boucke, R. R. Beerli, L. Vogt, C. Ruedl, M. F. Bachmann, U. F. Greber, and S. Hemmi.** 2004. The human membrane cofactor CD46 is a receptor for species B adenovirus serotype 3. J. Virol. **78:**4454–4462.
63. **Takeuchi, K., M. Takeda, N. Miyajima, F. Kobune, K. Tanabayashi, and M. Tashiro.** 2002. Recombinant wild-type and Edmonston strain measles viruses bearing heterologous H proteins: role of H protein in cell fusion and host cell specificity. J. Virol. **76:**4891–4900.
64. **Takikawa, S., K. Ishii, H. Aizaki, T. Suzuki, H. Asakura, Y. Matsuura, and T. Miyamura.** 2000. Cell fusion activity of hepatitis C virus envelope proteins. J. Virol. **74:**5066–5074.
65. **Tani, H., C. K. Limn, C. C. Yap, M. Onishi, M. Nozaki, Y. Nishimune, N. Okahashi, Y. Kitagawa, R. Watanabe, R. Mochizuki, K. Moriishi, and Y. Matsuura.** 2003. In vitro and in vivo gene delivery by recombinant baculoviruses. J. Virol. **77:**9799–9808.
66. **Tani, H., M. Nishijima, H. Ushijima, T. Miyamura, and Y. Matsuura.** 2001. Characterization of cell-surface determinants important for baculovirus infection. Virology **279:**343–353.
67. **Tatsuo, H., N. Ono, K. Tanaka, and Y. Yanagi.** 2000. SLAM (CDw150) is a cellular receptor for measles virus. Nature **406:**893–897.
68. **Tjia, S. T., G. M. zu Altenschildesche, and W. Doerfler.** 1983. *Autographa californica* nuclear polyhedrosis virus (*Ac*NPV) DNA does not persist in mass cultures of mammalian cells. Virology **125:**107–117.
69. **Volkman, L. E., and P. A. Goldsmith.** 1985. Mechanism of neutralization of budded *Autographa californica* nuclear polyhedrosis virus by a monoclonal antibody: inhibition of entry by adsorptive endocytosis. Virology **143:**185–195.
70. **Volkman, L. E., P. A. Goldsmith, R. T. Hess, and P. Faulkner.** 1984. Neutralization of budded *Autographa californica* NPV by a monoclonal antibody: identification of the target antigen. Virology **133:**354–362.
71. **Wu, Y., G. Liu, and E. B. Carstens.** 1999. Replication, integration, and packaging of plasmid DNA following cotransfection with baculovirus viral DNA. J. Virol. **73:**5473–5480.
72. **Zhang, S. X., Y. Han, and G. W. Blissard.** 2003. Palmitoylation of the *Autographa californica* multicapsid nucleopolyhedrovirus envelope glycoprotein GP64: mapping, functional studies, and lipid rafts. J. Virol. **77:**6265–6273.

Available online at www.sciencedirect.com
SCIENCE DIRECT®
Vaccine 23 (2005) 2269–2272
Vaccine
www.elsevier.com/locate/vaccine

The development of vaccines against SARS corona virus in mice and SCID-PBL/hu mice

Masaji Okada[a,*], Yuji Takemoto[a], Yoshinobu Okuno[b], Satomi Hashimoto[a], Shigeto Yoshida[c], Yukari Fukunaga[a], Takao Tanaka[a], Yoko Kita[a], Sachiko Kuwayama[a], Yumiko Muraki[a], Noriko Kanamaru[a], Hiroko Takai[a], Chika Okada[a], Yayoi Sakaguchi[a], Izumi Furukawa[a], Kyoko Yamada[a], Makoto Matsumoto[d], Tetsuo Kase[b], Daphne E. deMello[e], J.S.M. Peiris[f], Pei-Jer Chen[g], Naoki Yamamoto[h], Yoshiyuki Yoshinaka[h], Tatsuji Nomura[i], Isao Ishida[j], Shigeru Morikawa[k], Masato Tashiro[k], Mitsunori Sakatani[a]

[a] *Clinical Research Center, National Hospital Organization Kinki-Chuo Chest Medical Center, 1180 Nagasone, Sakai, Osaka 591-8555, Japan*
[b] *Department of Infectious Diseases, Osaka Prefectural Institute of Public Health, 3-69 Nakamichi 1-chome Higashinari-ku, Osaka 537-0025, Japan*
[c] *Department of Infection and Immunity, Jichi Medical School, 3311-1 Yakushiji, Minamikawachi-machi, Tochigi 329-0498, Japan*
[d] *Microbiological Research Institute, Otsuka Pharmaceutical Co., Ltd., 463-10, Kagasuno, Kawauchi-cho, Tokushima 771-019, Japan*
[e] *Department of Pathology Cardinal Glennon Children's Hospital, St. Louis University Health Science Center, 1465 South Grand Blvd. St. Louis, MO 63104, USA*
[f] *Department of Microbiology, The University of Hong Kong, Pokfulam Road, Hong Kong*
[g] *Hepatitis Research Center, National Taiwan University College of Medicine, Room 328, 3F, No.1, Sec. 1, Ren-ai Rd., Jhongjheng District 100, Taipei, Taiwan*
[h] *Tokyo Medical and Dental University, 1-5-45 Yushima, Bunkyo-ku, Tokyo 113-8549, Japan*
[i] *Central Institute for Experimental Animals, 1430 Nogawa, Miyamae, Kawasaki, Kanagawa 216-0001, Japan*
[j] *Pharmaceutical Division, Kirin Brewery Co., 6-26-1 Jingumae, Shibuya, Tokyo 150-8011, Japan*
[k] *National Institute of Infectious Diseases, 1-23-1 Toyama, Shinjuku-ku, Tokyo 162-8640, Japan*

Available online 21 January 2005

Abstract

We have investigated to develop novel vaccines against SARS CoV using cDNA constructs encoding the structural antigen; spike protein (S), membrane protein (M), envelope protein (E), or nucleocapsid (N) protein, derived from SARS CoV. Mice vaccinated with SARS-N or -M DNA using pcDNA 3.1(+) plasmid vector showed T cell immune responses (CTL induction and proliferation) against N or M protein, respectively. CTL responses were also detected to SARS DNA-transfected type II alveolar epithelial cells (T7 cell clone), which are thought to be initial target cells for SARS virus infection in human. To determine whether these DNA vaccines could induce T cell immune responses in humans as well as in mice, SCID-PBL/hu mice was immunized with these DNA vaccines. As expected, virus-specific CTL responses and T cell proliferation were induced from human T cells. SARS-N and SARS-M DNA vaccines and SCID-PBL/hu mouse model will be important in the development of protective vaccines.

Keywords: SARS DNA vaccine; SCID-PBL/hu; Human CTL

1. Introduction

The causative agent of severe acute respiratory syndrome (SARS) has been identified as a new type of corona virus, SARS corona virus (SARS CoV) [1–3]. SARS has infected more than 8400 patients in about 7 months in over 30 countries and caused more than 800 deaths. The deadly epidemic has had significant impacts on many health, social, economic and political aspects. SARS is assumed to resurge in the near future. However, no SARS vaccine is currently available for clinical use. Therefore, we have developed novel vaccine

* Corresponding author. Tel.: +81 72 252 3021; fax: +81 72 251 2153.
E-mail address: okm@kch.hosp.go.jp (M. Okada).

0264-410X/$ – see front matter © 2005 Elsevier Ltd. All rights reserved.
doi:10.1016/j.vaccine.2005.01.036

candidates against SARS CoV using cDNA constructs encoding the structural antigens; S, M, E, or N protein. In immunized mice, neutralizing antibodies against the virus and T cell immunity against virus-infected-cells were studied, since these immunities play important roles in protection against many virus infections. In particular, $CD8^+$ CTL plays an important role in T cell immunity dependent protection against virus infections and the eradication of murine and human cancers [4,5]. In the present study, a type II alveolar epithelial cell clone, T7, was used for analyzing precise mechanism of CTL against SARS CoV membrane antigens, as the SARS-CoV infects alveolar epithelial cell in the lungs [6]. Furthermore, the SCID-PBL/hu model, which is capable of analyzing in vivo human immune response, was also used because it is a more relevant translational model for human cases [4].

2. Materials and methods

Three kinds of SARS CoV strains: HKU39849(1), TW-1 and FFM-1(2) and their cDNAs were used. S, M, N or E cDNA was transferred into pcDNA 3.1(+) vector and pcDNA 3.1(+)/vs-His Topo (QIAGEN K K, Tokyo, Japan). These genes were expressed in eukaryotic cells and *Escherichia coli*. pcDNA 3.1(+) vector, 50 μg each, containing SARS S, M, N, or E DNA was injected i.m. (M.tibia anterior) into C57BL/6 mice (female, 8 weeks CLEA Japan Inc, Japan) and BALB/c mice (female, 8 weeks) three times, at an interval of 7 days. Neutralizing antibodies against SARS CoV in the serum from the mice immunized with SARS S, M, N or -E DNA vaccines were assayed by use of Vero-E6 cell. CTL activity against SARS CoV was studied using human type II alveolar epithelial cells, T7, expressing SARS antigens [6]. PBL from healthy human volunteers were administered i.p. into IL-2 receptor γ-chain disrupted NOD SCID mice [IL-2R(−/−) NOD-SCID], and SCID-PBL/hu mice were constructed [4]. SARS DNA vaccines at 50 μg were injected i.m. into the SCID-PBL/hu mice. CTL activity of human CD8-positive lymphocytes in the spleen from SCID-PBL/hu was assessed using IFN-γ production and 51Cr-release assay [4,5].

3. Results

3.1. Induction of CTL against SARS CoV by SARS (N) DNA and SARS (M) DNA vaccine

Spleen cells from C57BL/6 mice immunized with SARS-S, -M, -N or -E DNA vaccine were cultured with syngeneic T7 lung cells transfected with S, M, N or E cDNA. pcDNA 3.1(+) SARS (N) DNA vaccine induced significantly CTL activity (IFN-γ production) against N cDNA transfected T7 cells (Fig. 1A). Similarly, SARS M DNA vaccine induced SARS antigen M-specific CTL against T7 cells transfected with SARS M DNA (data not shown).

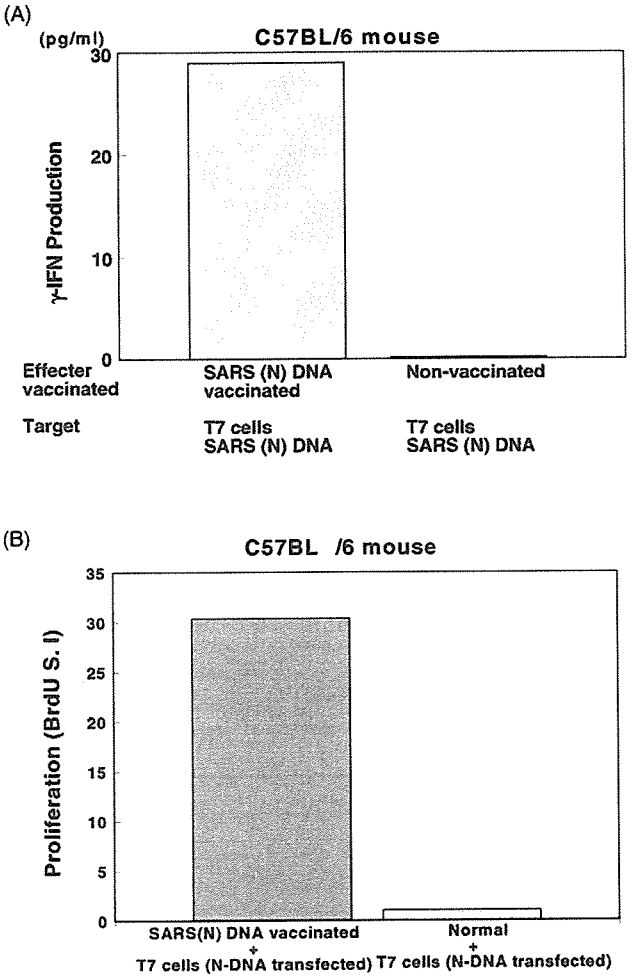

Fig. 1. Induction of CTL and T cell proliferation against SARS (N). (A) Induction of CTL against SARS (N) antigen in the spleen cells from C57BL/6 mice immunized with SARS (N) DNA vaccine. SARS (N) DNA using pcDNA3.1(+) vector was injected i.m. into C57BL/6 mice three times, at an interval of 7 days. CTL activity was assessed by IFN-γ production in the culture of 1×10^6 spleen cells and 1×10^4 T7 lung alveolar type II epithelial cells transfected with SARS (N) DNA at the E/T ratio of 100:1. IFN-γ production was assessed by ELISA assay. (B) Augmentation of lymphocyte proliferation specific for SARS (N) DNA vaccine. 1×10^5 responder cells from vaccinated mice were cultured with Mitomycin C treated 1×10^4 T7 cells transfected with SARS (N) DNA for 48 h and then Bromodeoxy Uridine (BrdU) was added. Proliferative responses were assessed by BrdU assay.

3.2. Augmentation of lymphocyte proliferation specific for SARS CoV antigens by the immunization with SARS (M) DNA and SARS (N) DNA vaccine

The proliferation of splenic T cells stimulated by co-culture either with T7 cells transfected with M DNA or SARS M peptide (TW1 M102-116) was strongly augmented by M DNA vaccine (data not shown). SARS N DNA vaccine also induced proliferation of splenic T cells in the presence of recombinant N protein as well as N DNA-transfected T7 cells (Fig. 1B). Thus, both SARS N DNA vaccine and

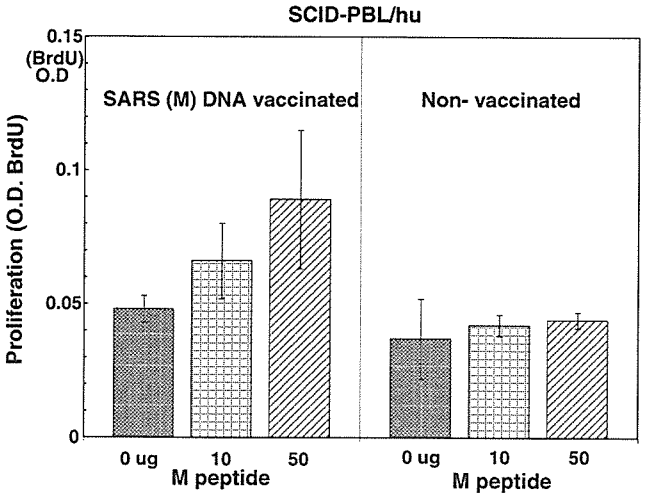

Fig. 2. SARS (M) DNA vaccine induces in vivo human T cell proliferation against SARS CoV in the SCID-PBL/hu human immune systems. 4×10^7 PBL from healthy human volunteers were administered i.p. into IL-2 receptor γ-chain disrupted NOD SCID mice [IL-2R (−/−) NOD-SCID], and SCID-PBL/hu mice were constructed. Fifty micrograms of SARS DNA vaccine was injected i.m. into these SCID-PBL/hu mice. 1×10^5 spleen cells from these vaccinated mice were cultured with 10~50 μg of SARS M peptide for 3 days. Proliferation was assayed by BrdU.

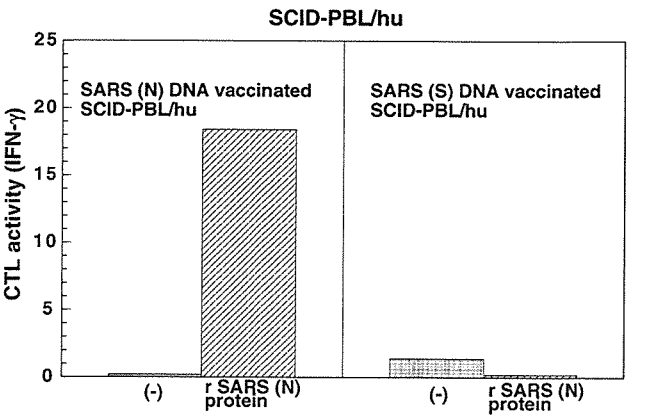

Fig. 3. SARS (N) DNA vaccine induces in vivo human CTL against SARS CoV in the SCID-PBL/hu human immune systems. 4×10^7 PBL from healthy human volunteers were administered i.p. into IL-2 receptor γ-chain disrupted NOD SCID mice [IL-2R (−/−) NOD-SCID], and SCID-PBL/hu mice were constructed 50 μg of SARS (N) DNA vaccine or 50 μg of SARS (S) DNA vaccine. 1×10^5 spleen cells from SCID-PBL/hu were cultured with 10 μg of recombinant SARS (N) protein for 72 h. IFN-γ production in the culture supernatant was assayed using ELISA.

M DNA vaccine were shown to induce T cell immune responses against the relevant SARS CoV antigens.

3.3. SARS M DNA and N DNA vaccines induced human T cell immune responses (CTL and proliferation) in SCID-PBL/hu model

The M DNA vaccine enhanced the CTL activity and proliferation in the presence of M peptide in SCID-PBL/hu mice (Fig. 2). Furthermore, the SARS N DNA vaccine induced CTL activity (IFN-γ production by recombinant N protein or N protein pulsed-autologous B blast cells) and proliferation of spleen cells in SCID-PBL/hu mice (Fig. 3). From these results, it was demonstrated that SARS M DNA vaccine and N DNA vaccine induced human CTL and human T cell proliferative responses.

4. Discussion

We have demonstrated that SARS (M) DNA and (N) DNA vaccines induce virus-specific immune responses (CTL and T cell proliferation) in the mouse systems using type II lung alveolar T cell lines in clone target models [6]. These DNA vaccines induced SARS-CoV-specific CTL and T cell proliferation in vivo human immune systems using SCID-PBL/hu. Gao et al. developed adenovirus based a SARS DNA vaccine encoding S1 polypeptide was capable of inducing neutralizing antibody, while another SARS DNA vaccine encoding N protein generated IFN-γ producing T cells in rhesus monkeys [7]. SARS S DNA vaccine which elicits effective neutralizing antibody responses that generate protective immunity in a mouse model [8]. However its immunogenicity in humans has yet to be established. Therefore, it is very important to evaluate the efficacy of SARS DNA vaccine in a SCID-PBL/hu mice, which is a highly relevant translational model for demonstrating human immune responsiveness. Recently, SARS DNA vaccines capable of inducing human neutralizing antibodies against SARS CoV have been established by our SCID-PBL/hu model. It has been demonstrated that Angiotensin-converting enzyme 2 (ACE2) is a functional receptor for the SARS CoV [9]. A transgenic mouse with human ACE-2 may be useful as an animal model of SARS. Furthermore, ACE-2 transgenic SCID mice should be useful as a human model for pre-clinical trial for SARS vaccines, since ACE-transgenic SCID-PBL/hu model could analyze the human immune responses against SARS infection in vivo. The effect of combination immunization with such SARS vaccines and neutralizing antibody dependent DNA vaccine is now being studied. These DNA vaccines should provide a useful tool for development of protective vaccines.

Acknowledgements

This study was supported by Grant-in-Aid for the science and technology and Grant-in-Aid for Scientific Research on Priority Areas from the Ministry of Education Culture Sports, Science and Technology, Japan. This study was also supported by a Heath and Labour Science Research Grant from the Ministry of Health, Labour, and Welfare, Japan.

References

[1] Peiris JS, Lai ST, Poon LL, Guan Y, Yam LY, Lim W, et al. SARS study group. Coronavirus as a possible cause of severe acute respiratory syndrome. Lancet 2003;361(9366):1319–25.

[2] Drosten C, Gunther S, Preiser W, van der Werf S, Brodt HR, Becker S, et al. Identification of a novel coronavirus in patients with severe acute respiratory syndrome. N Engl J Med 2003;348(20):1967–76.
[3] Peiris JS, Yuen KY, Osterhaus AD, Stohr K. The severe acute respiratory syndrome. N Engl J Med 2003;349(25):2431–41.
[4] Tanaka F, Abe M, Akiyoshi T, Nomura T, Sugimachi K, Kishimoto T, et al. The anti-human tumor effect and generation of human cytotoxic T cells in SCID mice given human peripheral blood lymphocytes by the in vivo transfer of the Interleukin-6 gene using adenovirus vector. Cancer Res 1997;57(7):1335–43.
[5] Okada M, Yoshimura N, Kaieda T, Yamamura Y, Kishimoto T. Establishment and characterization of human T hybrid cells secreting immunoregulatory molecules. Proc Natl Acad Sci USA 1981;78(12):7717–21.
[6] deMello DE, Mahmoud S, Padfield PJ, Hoffmann JW. Generation of an immortal differentiated lung type-II epithelial cell line from the adult H-2K(b)tsA58 transgenic mouse. In Vitro Cell Dev Biol Anim 2000;36(6):374–82.
[7] Gao W, Tamin A, Soloff A, D'Aiuto L, Nwanegbo E, Robbins PD, et al. Effects of a SARS-associated coronavirus vaccine in monkeys. Lancet 2003;362(9399):1895–6.
[8] Yang ZY, Kong WP, Huang Y, Roberts A, Murphy BR, Subbarao K, et al. A DNA vaccine induces SARS coronavirus neutralization and protective immunity in mice. Nature 2004;428(6982):561–4.
[9] Li W, Moore MJ, Vasilieva N, Sui J, Wong SK, Berne MA, et al. Angiotensin-converting enzyme 2 is a functional receptor for the SARS coronavirus. Nature 2003;426(6965):450–4.

Protease-mediated enhancement of severe acute respiratory syndrome coronavirus infection

Shutoku Matsuyama*, Makoto Ujike*, Shigeru Morikawa†, Masato Tashiro*, and Fumihiro Taguchi*‡

Division of Respiratory Viral Diseases and SARS, *Department of Virology III, Special Pathogens Laboratory, †Department of Virology I, National Institute of Infectious Diseases, Murayama Branch, Gakuen 4-7-1, Musashi-Murayama, Tokyo 208-0011, Japan

Edited by Peter Palese, Mount Sinai School of Medicine, New York, NY, and approved July 19, 2005 (received for review April 19, 2005)

A unique coronavirus severe acute respiratory syndrome-coronavirus (SARS-CoV) was revealed to be a causative agent of a life-threatening SARS. Although this virus grows in a variety of tissues that express its receptor, the mechanism of the severe respiratory illness caused by this virus is not well understood. Here, we report a possible mechanism for the extensive damage seen in the major target organs for this disease. A recent study of the cell entry mechanism of SARS-CoV reveals that it takes an endosomal pathway. We found that proteases such as trypsin and thermolysin enabled SARS-CoV adsorbed onto the cell surface to enter cells directly from that site. This finding shows that SARS-CoV has the potential to take two distinct pathways for cell entry, depending on the presence of proteases in the environment. Moreover, the protease-mediated entry facilitated a 100- to 1,000-fold higher efficient infection than did the endosomal pathway used in the absence of proteases. These results suggest that the proteases produced in the lungs by inflammatory cells are responsible for high multiplication of SARS-CoV, which results in severe lung tissue damage. Likewise, elastase, a major protease produced in the lungs during inflammation, also enhanced SARS-CoV infection in cultured cells.

cell entry | protease | spike protein | SARS

Severe acute respiratory syndrome (SARS) is caused by a SARS-associated coronavirus (SARS-CoV), a newly emergent member in a family of Coronaviridae (1–6). Unlike other human coronaviruses, SARS-CoV causes a fatal respiratory disease in humans (1–6). Coronavirus is an enveloped virus with a positive-stranded large genomic RNA with ≈30 kb (7). Spikes exist on the virion surface and resemble solar corona, each of which is composed of a trimer of the spike (S) protein (7, 8). The S protein is a type I fusion protein of an approximate molecular weight of 180 kDa. The prototypical coronavirus mouse hepatitis virus enters into cells via the cell surface, although a variant isolated from persistent infection enters from an endosome, the low pH of which induces its fusion activity (9). However, the entry pathway of SARS-CoV appears to be distinct from that of the other coronaviruses. Simmons *et al.* (10) hypothesized that SARS-CoV enters cells by an endosomal pathway, and S protein is activated for fusion by trypsin-like protease in an acidic environment. This idea is based on the following two findings: (*i*) SARS-CoV infection can be blocked by lysosomotropic agents, and (*ii*) S protein expressed on cells is activated for fusion by trypsin. These results were obtained by studies using pseudotype retroviruses harboring SARS-CoV S protein on the envelope and those using S protein expressed on cells by expression vectors (10).

In the present study, we show that various proteases, as well as trypsin, are effective in inducing the fusion of SARS-CoV-infected VeroE6 cells. These proteases facilitated SARS-CoV entry from the cell surface, which indicates that SARS-CoV has the potential to enter cells via two different pathways, either an endosomal or a nonendosomal pathway, depending on the presence of proteases. More interestingly, SARS-CoV entry from cell surface mediated by protease resulted in >100-fold more efficient infection than entry through endosome. Elastase, a major protease produced during lung inflammation, also manifested this enhancing effect. These findings suggest that severe illness in the lungs and intestines is attributable to the proteases produced in these organs during an inflammatory response or in the presence of certain physiological conditions.

Materials and Methods

Cells and Viruses. VeroE6 cells were grown in DMEM (Nissui, Tokyo), supplemented with 5% FBS (GIBCO/BRL). The SARS-CoV Frankfurt 1 strain, kindly provided by J. Ziebuhr (University of Würzburg, Würzburg, Germany) (1), was propagated and assayed by using Vero E6 cells.

Proteases. Various proteases were dissolved in PBS (pH 7.2) and used at the indicated concentrations in DMEM containing 5% FCS. The proteases used in this study were trypsin (Sigma, T-8802), thermolysin (Sigma, P 1512), chymotrypsin (Sigma, C-3142), dispase (Roche, 1 276 921), papain (Worthington, 53J6521), proteinase K (Wako, Tokyo), collagenase (Sigma, C-5183), and elastase (Sigma, E-0258).

Plaque Assay. VeroE6 cells prepared in 24-well plates were inoculated with 50 μl of 10-fold serially diluted virus samples and incubated at 37°C for 1 h. Cells were then cultured with 0.5 ml per well of DMEM containing 1% FCS and 0.75% methyl cellulose (Sigma) for 2 d. Cells were fixed with 1 ml of 10% formaldehyde per well for at least 2 h. After removing the culture fluids, cells were irradiated overnight under a UV lamp and stained with crystal violet. Plaques produced by SARS-CoV were counted under light microscopy. Titration was done in duplicate and infectivity was displayed by plaque-forming units (pfu).

Western Blotting. S protein expressed in Vero E6 cells was analyzed by Western blotting. Preparation of cell lysates, SDS/PAGE, and electrical transfer of the protein onto a transfer membrane were described (11). S protein was detected with anti-S Ab, IMG-557 (Imgenex, San Diego) and horseradish peroxidase-conjugated anti-rabbit IgG Ab (anti-R-IgG, ALI3404, BioSource International, Camarillo, CA). The bands were visualized by using enhanced chemiluminescence reagents (ECL-plus, Amersham Pharmacia) on a LAS-1000 instrument (Fuji).

Real-Time PCR. VeroE6 cells in 96-well culture plates were treated with DMEM containing 1 μM bafilomycin (Baf; Sigma, B-1793) and 5% FCS (DMEM plus Baf) at 37°C for 30 min and then chilled on ice for 10 min. Approximately 10^4 pfu of virus in DMEM plus Baf were infected to 10^4 cells on ice; multiplicity of

This paper was submitted directly (Track II) to the PNAS office.

Abbreviations: SARS-CoV, severe acute respiratory syndrome-coronavirus; S, spike; pfu, plaque-forming unit; moi, multiplicity of infection; Baf, bafilomycin.

‡To whom correspondence should be addressed. E-mail: ftaguchi@nih.go.jp.

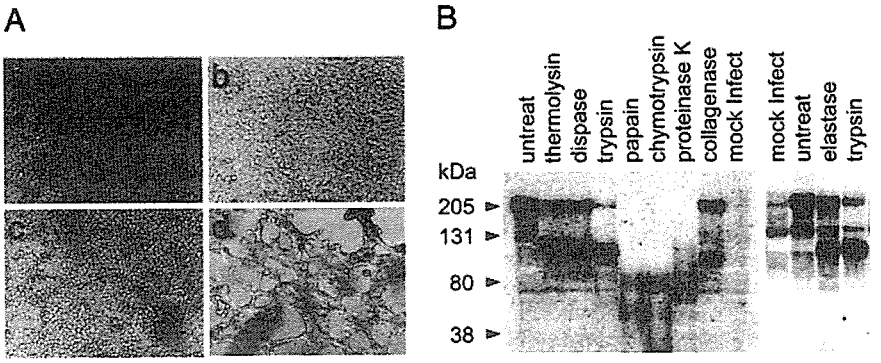

Fig. 1. Induction of cell-fusion and SARS-CoV S protein cleavage by proteases. (*A*) Syncytium formation after treatment with trypsin. VeroE6 cells cultured in 24-well plates were infected (*b* and *d*) or mock-infected (*a* and *c*) with the SARS-CoV Frankfurt 1 strain at moi = 0.5 and incubated at 37°C for 20 h. Cells were washed once with PBS and treated (*c* and *d*) or untreated (*a* and *b*) with 200 μg/ml trypsin for 5 min. Those cells were cultured for a further 4 h and observed by microscopy. (*B*) Western blot analysis of S protein treated with various proteases. Cells infected as described above were treated either with thermolysin (200 μg/ml), dispase (1 unit/ml), trypsin (200 μg/ml), papain (0.74 unit/ml), chymotrypsin (1 mg/ml), proteinase K (8 μg/ml) collagenase (200 μg/ml), or elastase (1 mg/ml), as described above. Soon after treatment, cells were lysed with lysing buffer, and S protein was analyzed by Western blot after SDS/PAGE. To detect the S protein (S2 fragment), mAb IMG-557 was used at a concentration of 5 μg/ml.

infection (moi) was at 1. After 30-min adsorption, the virus was removed, and infected cells were treated for 5 min with various concentrations of proteases in DMEM plus Baf that was prewarmed at room temperature. After protease was removed, cells were cultured in DMEM plus Baf at 37°C for 6 h. Vero E6 cell monolayers in 24-well plates were infected with 10 pfu of SARS-CoV (moi = 0.0001). After 30-min adsorption, cells were cultured in DMEM containing 5% FCS in the presence or in the absence of various proteases for 20 h. To isolate cellular RNA, 100 and 500 μl of isogen (Nippon Gene, Toyama, Japan) were added to each well of 96- and 24-well plates, respectively, together with 5 μg of yeast RNA as a carrier for 2-propanol precipitation. RNA was prepared according to the manufacturer's instructions and finally dissolved in 20 μl of diethyl pyrocarbonate-treated water. Real-time PCR was performed to estimate the amounts of mRNA9 in a final volume of 20 μl of 1× LightCycler RNA Master Mix (Roche Diagnostics) by using the RNA isolated as described above. For amplification of the fragment from mRNA9, we used 500 nM of a pair of oligonucleotides 5′-CTCGATCTCTTGTAGATCTG-3′ (SARS leader) and 5′-TCTAAGTTCCTCCTTGCCAT-3′ (SARS mRNA9 reverse). Amplified DNA from mRNA has 240 bases. With these primers, genomic RNA was not detected because the fragment to be amplified from genomic RNA would be ≈30 kb. For detection by hybridization, 200 nM each of the hybridization probes 5′-ACCAGAATGGAGGACGCAATGGGGCAAG-3′ (3′FITC labeled), 5′-CCAAAACAGCGCCGACCCCAAGGTTTAC-3′ (5′LCRed640 labeled) were used. PCR analysis was performed under the following conditions [reverse transcription: 61°C, 20 min; PCR, 95°C, 30 s (95°C, 5 s; 55°C, 15 s; 72°C, 10 s) ×45 cycles] with a LightCycler instrument (Roche Diagnostics). To measure the amounts of viruses that entered into cells, we infected cells with 10-fold stepwise diluted SARS-CoV from 10^6 to 10^2 pfu, and the amounts of mRNA9 were determined by real-time PCR. The amounts of virus that entered into cells after protease treatment were calculated from a calibration line obtained as above and shown as relative mRNA levels. When relative mRNA9 was higher than 10^6 pfu, samples were diluted and reexamined so that they were placed between 10^6 and 10^2 pfu.

Results

Activation of Cell Fusion and SARS-CoV S Protein Cleavage by Various Proteases. VeroE6 cells susceptible to SARS-CoV were infected with the Frankfurt-1 strain of SARS-CoV at a moi of 0.5, and those infected cells were treated with trypsin at 20 h after infection. Cell fusion was detected from 2 h after trypsin treatment (Fig. 1*Ad*). Fusion was also found after treatment with thermolysin or dispase (data not shown). Little or no fusion occurred after treatment with papain, chymotrypsin, proteinase K, or collagenase. S proteins in cells treated with proteases that induce fusion were cleaved approximately in the middle (Fig. 1*B*), a finding similar to that of Simmons *et al.* (10). In contrast, no apparent S2 band was detected in cells bearing S proteins treated with proteases that failed to induce fusion (Fig. 1*B*). These results showed that various proteases, including trypsin, activate the fusion activity of the SARS-CoV S protein by inducing its cleavage. Further, SARS-CoV infection was extensively inhibited by treatment of cells with Baf (Fig. 2*A*, no Baf vs. Baf without protease). These results suggest that SARS-CoV takes an endosomal pathway for its entry, and that S protein cleavage is important for fusogenicity, which is consistent with the conclusions of a previous report (10).

SARS-CoV Entry from Cell Surface Facilitated by Proteases. If the hypothesis proposed by Simmons *et al.* (10) is correct, we can make SARS-CoV enter cells directly from their surface by attaching the virus there and treating them with trypsin and other proteases that induce fusion. Treatment of VeroE6 cells with Baf at a concentration of 1 μM suppressed SARS-CoV infection via the endosomal pathway to <1/100, as shown in Fig. 2*A*. The cells treated with Baf were inoculated with SARS-CoV at a moi of 1 and incubated on ice for 30 min (adsorption on ice does not allow virus to enter cells). Then cells were treated with various proteases for 5 min at room temperature and incubated at 37°C for 6 h. Virus entry was estimated by the newly synthesized mRNA9 measured quantitatively by real-time PCR. A calibration curve of real-time PCR (Fig. 2*C*), showing the level of mRNA9 after infection with 10-fold diluted SARS-CoV, was used to estimate the amount of infected virus from the mRNA levels. As shown in Fig. 2*A*, thermolysin and trypsin, two proteases with fusion-inducing activity, extensively facilitated viral entry. In contrast, two proteases that did not induce fusion, papain and collagenase failed to do so. Treatment of cells with trypsin before virus infection did not facilitate viral entry (Fig. 2*B*), indicating that effects of trypsin on cells are not involved in this infection. Other proteases did not influence the SARS-CoV infection as trypsin, when treated before virus inoculation (data not shown). Protease treatment of SARS-CoV before infection did not enhance infectivity but reduced it by 10- to 100-fold (data

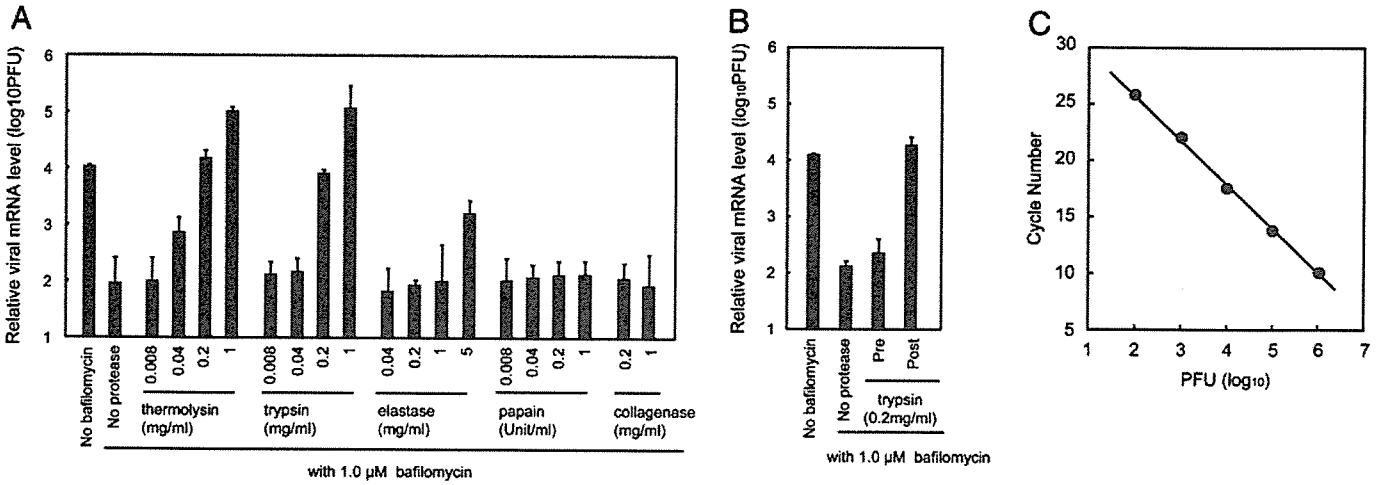

Fig. 2. Entry of SARS-CoV from cell surface facilitated by proteases. (*A*) Effect of proteases on SARS-CoV entry into VeroE6 cells treated with Baf. VeroE6 cells in 96-well plates were treated with Baf at a concentration of 1 μM at 37°C for 30 min, placed on ice and infected with SARS-CoV at moi = 1 for 30 min. Then, cells were treated with various concentrations of different proteases at room temperature for 5 min and cultured in the presence of Baf for a further 6 h. The amount of mRNA9 was measured quantitatively by real-time PCR. Cells untreated with Baf or those treated with Baf but untreated with protease were used as controls. The relative viral mRNA level is displayed by virus infectivity (pfu) calculated from a calibration line shown in *C*. (*B*) Cells treated with Baf at 37°C for 30 min were then treated with trypsin at room temperature for 5 min before (pre) or after (post) virus inoculation, and virus infection was estimated quantitatively by real-time PCR as described above. (*C*) Calibration in real-time PCR. VeroE6 cells in 94-well plates were infected with 10-fold step diluted viruses, and mRNA9 levels at 6 h after infection were estimated by real-time PCR. The relationship is shown between inoculated pfu (*x* axis) and cycles of real-time PCR to reach a positive level (amount of mRNA9) (*y* axis).

not shown). We believe these results demonstrate that SARS-CoV, when adsorbed onto the cell surface, fuse with the plasma membrane of its envelope with S protein, which is cleaved into S1 and S2 by proteases with fusion-inducing activity. This suggests a nonendosomal, direct entry of SARS-CoV into cells in the presence of proteases. Those findings also support the hypothesis drawn by Simmons *et al.* (10) that trypsin-like protease plays an important role in facilitating membrane fusion.

Enhancement of SARS-CoV Infection by Various Proteases. Treatment with a high concentration of thermolysin and trypsin augmented virus entry or replication by 10-fold or higher, as compared with the standard infection (Fig. 2*A*, e.g., compare bar 6 or bar 10 with bar 1 from the left). We then compared the replication kinetics of SARS-CoV in cells treated with Baf and a high concentration of trypsin with that of cells maintained without Baf or trypsin. The level of mRNA9 was always ≈10-fold higher in trypsin-treated cells at any given time during the early period of infection (Fig. 3). These data also imply that viral replication after entry via the cell surface proceeds ≈1 h ahead of that via the endosomal pathway, suggesting that the surface route is more efficient for rapid viral replication.

Because SARS-CoV replication was shown to be enhanced by trypsin treatment, we next assessed the efficiency of virus spread in the presence or absence of trypsin in a low moi, which mimics natural infection in target organs. Virus (10 pfu) were inoculated onto 10^5 confluent VeroE6 cells (moi = 0.0001), and the cells were incubated at 37°C for 20 h in the media with or without trypsin. The level of mRNA9 estimated quantitatively by real-time RT-PCR showed that virus replication was 100- to 1,000-fold higher when cells were cultured in the presence of trypsin, when compared with replication in the absence of trypsin (Fig. 4*A*). Viral infectivity of the supernatants in SARS-CoV-infected cells cultured with or without trypsin also indicated that trypsin treatment enhanced viral growth by ≈100-fold (Fig. 4*B*). We also examined growth kinetics of SARS-CoV in the presence of low-concentration proteases (62.5 μg/ml trypsin, 125 μg/ml elastase) that do not detach cells from plates during culture for 42 h. It was also shown that protease enhanced virus replication (Fig. 4*C*) with remarkable fusion formation (Fig. 4*D*). All of these results strongly suggest that the virus spreads efficiently from cell to cell in the presence of trypsin, which cleaves S to S1 and S2 to allow cell entry of SARS-CoV via the cell surface.

We next examined the effects on low moi by other proteases that facilitate SARS-CoV entry from VeroE6 cell surface. As shown in Fig. 5, all of the proteases that produce S2 (Fig. 1*B*) and that induce cell-cell fusion enhanced virus spread. In contrast, those proteases that did not generate S2 and that did not induce cell-cell fusion failed to enhance the infection. These observations suggest that proteases that facilitate SARS-CoV entry from the cell surface support efficient SARS-CoV infection. Thus, protease is likely to be responsible for the high multiplication of

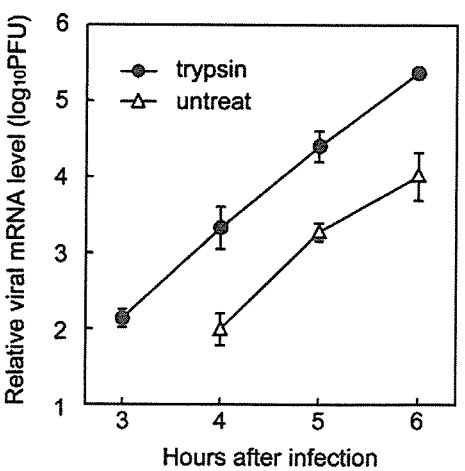

Fig. 3. Kinetics of mRNA9 synthesis after treatment of trypsin. VeroE6 cells were treated with Baf, infected with SARS-CoV, and treated with 200 μg/ml trypsin as described in the legend to Fig. 2*A*. The amount of mRNA9 synthesized was monitored by real-time PCR at 3–6 h after inoculation. VeroE6 cells without any treatment were also infected as a control (untreated). Relative viral mRNA level is displayed by virus infectivity (pfu) calculated from the calibration line shown in Fig. 2*C*.

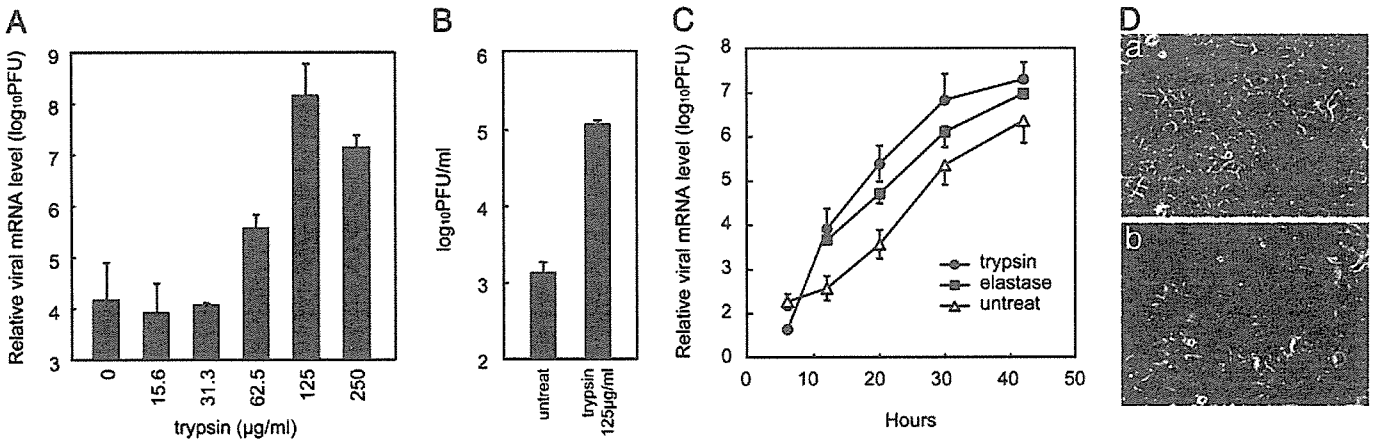

Fig. 4. Enhancement of SARS-CoV infection by proteases. (*A*) Effect of trypsin on virus replication in VeroE6 cells. Approximately 1×10^5 VeroE6 cells cultured in 24-well plates were infected with 10 pfu of SARS-CoV (moi = 0.0001) and cultured in the presence of varied trypsin concentrations. Viral replication was estimated at 20 h after infection by the amount of mRNA9, as measured by real-time PCR. (*B*) Viral infectivity was examined by plaque assay after 20-h incubation in the presence or absence of trypsin (125 μg/ml). (*C*) Viral growth kinetics after infection was examined in cultures in the presence or absence of trypsin (62.5 μg/ml) or elastase (125 μg/ml) by real-time PCR. Cells were harvested from 4 to 42 h after infection at intervals and the level of mRNA9 was monitored. Relative viral mRNA level is displayed by virus infectivity (pfu) calculated from a calibration line (*A–C*). (*D*) Cytopathic changes of virus-infected cells cultured in the presence (*b*) or absence (*a*) of trypsin (125 μg/ml) for 42 h are shown.

SARS-CoV in the major target organs of SARS, such as the lungs and bronchus, where various proteases are produced (e.g., by inflammatory cells), as well as in the intestines, where a number of proteases are physiologically secreted.

One of the major proteases produced by inflammatory cells in the lungs is an elastase produced by neutrophils (12), the accumulation of which was reported in the lungs of SARS patients (13). The level of elastase in bronchoalveolar lavage fluids was reported to reach levels as high as 700 μg/ml (12). Accordingly, we determined whether this protease has the potential to enhance SARS-CoV infection in a fashion similar to that of trypsin or thermolysin. Elastase was revealed to enhance SARS-CoV infection in cultured VeroE6 cells in terms of S protein cleavage (Fig. 1*B*), its cell-surface-mediated entry pathway (Fig. 2*A*), and its growth enhancement ability after low moi

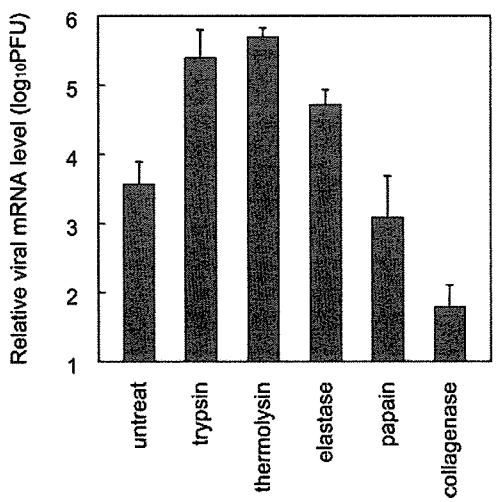

Fig. 5. Effect of various proteases on virus replication in VeroE6 cells. VeroE6 cells in 24-well plates were infected as described in Fig. 4 and cultured in the presence of trypsin (62.5 μg/ml), thermolysin (12.5 μg/ml), elastase (125 μg/ml), papain (0.037 unit/ml), or collagenase (200 μg/ml). At 20 h after infection, the amounts of mRNA9 were measured by real-time PCR. Relative viral mRNA level is displayed by virus infectivity (pfu) calculated from the calibration line.

(Figs. 4*C* and 5). These results strongly suggest that SARS-CoV replication can be enhanced in the lungs by elastase.

Discussion

The SARS-CoV gene and viral antigens were found in a number of organs, such as the liver, cerebrum, pancreas, and kidneys, as well as in such major target organs as the bronchus, lungs, and intestines (14–17), with the latter showing drastic tissue damage by SARS-CoV infection, whereas the other organs were not so severely affected. Although the pathogenic mechanism of SARS has not been elucidated, the present study suggests that proteases secreted in major target organs play an important role in the high multiplication of virus in those organs, which, in turn, results in severe tissue damage. An initial infection by SARS-CoV in pneumocytes via its receptor ACE2 (18), the endosomal pathway, could induce inflammation that generates a variety of proteases such as elastase. Once those proteases are present in the lungs, they may mediate an ensuing robust infection, which may result in enhanced replication of SARS-CoV in the lungs. Although lung damage is postulated to be mediated by cytokines by a so-called cytokine storm (14, 16), higher virus multiplication could also contribute to the cytokine storm by killing a large number of infected cells. A variety of proteases secreted in the small intestines, another major target organ of SARS-CoV, could also be responsible for the high growth of SARS-CoV in these tissues, which could result in a high rate of diarrhea in SARS patients (19, 20).

Protease-mediated enhancement of infection is known for orthomyxovirus and paramyxovirus infections (21–24), in which their envelope glycoprotein is not fully cleaved in *de novo* synthesized cells, and thus the virus particles produced contain partially cleaved or uncleaved glycoprotein. Those glycoproteins on virions are cleaved after treatment with protease, which results in the enhancement of infectivity. Thus, trypsin affects directly virons and increases the infectivity of those viruses. However, enhancement of SARS-CoV infection by trypsin or other proteases is mediated by another mechanism. Although trypsin treatment *in vitro* induces cleavage of the S protein on virions, such treatment never enhances SARS-CoV infectivity but reduces it to 1/10–1/100 of the original titer. Only S protein bound to its receptor ACE2 and cleaved by proteases could obtain fusion activity. Based on this idea, it is most likely that

binding of S protein to ACE2 induces conformational changes of the S, which is inevitable to be correctly processed for fusion activity by proteases. In other words, proteases can successfully induce the fusion activity of S protein only after S-ACE2 binding. Alternatively, protease treatment of virions digests out the S1 portion important for ACE2 binding, resulting in a loss of infectivity, whereas S2 alone is sufficient for fusion after binding to its receptor despite loss of the S1 fragment.

Why is the infection via the endosomal pathway not as efficient as direct infection from the cell surface? Throughout our examinations, replication deriving from the cell surface pathway began 1 h ahead of that via the endosomal pathway. We assume that a virus needs ≈1 h for trafficking from the cell surface where virion binds to ACE2 to the endosome. When cells are infected with an extremely low moi, a condition that occurs in natural infection, a 100- to 1,000-fold higher rate of infection was observed in the presence of proteases. Thus a 10-fold difference at 6 h after inoculation could result in a 1,000-fold difference, provided that one cycle of SARS-CoV replication is ≈6 h (25) and three rounds of infection take place within 20 h.

The present studies suggest that coinfection of SARS-CoV with some other non- or low-pathogenic respiratory agents, such as *Chlamydia*, mycoplasma, or bacteria, results in severe lung disease, which is attributed to the proteases produced by the infection with those non-SARS-CoV agents, as has been shown by the enhancement of respiratory diseases caused by influenza virus coinfected with nonpathogenic bacteria (26, 27). Studies are in progress to see whether coinfection exacerbates pneumonia in mice infected with SARS-CoV.

We thank Miyuki Kawase for excellent technical assistance throughout the experiments, John Ziebuhr (University of Würzburg, Würzburg, Germany) for providing SARS-CoV Frankfurt-1, and Judith White (University of Virginia, Charlottesville) for valuable comments on this work. We also thank the colleagues of our institute, especially Shuetsu Fukushi, Keiko Nakagaki, Kohji Ishii, and Yasuko Yokota, for valuable discussions and encouragement throughout the research. This work was supported by Ministry of Education, Culture, Sports, Science, and Technology Grant 16017308 and Ministry of Health, Labor, and Welfare Grant H16-Shinkoh-9.

1. Ksiazek, T .G., Erdman, D., Goldsmith, C., Zaki, S. R., Peret, T., Emery, S., Tong, S., Urbani, C., Comer, J. A., Lim, W., *et al.* (2003) *N. Engl. J. Med.* **348,** 1953–1966.
2. Drosten, C., Gunther, S., Preiser, W., Van Der Werf, S., Brodt, H. R., Becker, S., Rabenau, H., Panning, M., Kolesnikowa, L., Fouchier, R. A., *et al.* (2003) *N. Engl. J. Med.* **348,** 1967–1976.
3. Marra, M. A., Jones, S. J., Astell, C. R., Holt, R. A., Brooks-Wilson, A., Buttefield, Y. S., Khattra, J., Asano, J. K., Barber, S. A., Chan, S. Y., *et al.* (2003) *Science* **300,** 1399–1404.
4. Rota, P. A., Oberste, M. S., Monroe, S. S., Nix, W. A., Campagnoli, R., Icenogle, J. P., Penaranda, S., Bankamp, B., Maher, K., Chen, M. H., *et al.* (2003) *Science* **300,** 1394–1399.
5. The Chinese SARS Molecular Epidemiology Consortium (2004) *Science* **303,** 1666–1669.
6. Peiris, J. S., Guan, Y. & Yuen, K. Y. (2005) *Nat. Med.* **10,** 588–597.
7. Lai, M. M. C. & Cavanagh, D. (1997) *Adv. Virus Res.* **48,** 1–100.
8. Tyrell, D. A. J., Almeida, J. D., Berry, D. M., Cunningham, C. H., Hamre, D., Hofstad, M. S., Mallucci, L. & McIntosh, K. (1968) *Nature* **220,** 650.
9. Gallagher, T. M., Escarmis, C. & Buchmeier, M. J. (1991) *J. Virol.* **65,** 1916–1928.
10. Simmons, G., Reeves, J. D., Rennekamp, A. J., Amberg, S. M., Piefer, A. J. & Bates, P. (2004) *Proc. Natl. Acad. Sci. USA* **101,** 4240–4245.
11. Matsuyama, S. & Taguchi, F. (2000) *Virology* **273,** 80–89.
12. Kawabata, K., Haio, T. & Matsuoka, S. (2002) *Eur. J. Pharmacol.* **451,** 1–10.
13. Wong, C. K., Lam, C. W., Wu, A. K., Ip, W. K., Lee, N. L., Chan, I. H., Lit, L. C., Hui, D. S., Cha, M. H., Chung, S. S., *et al.* (2004) *Clin. Exp. Immunol.* **136,** 95–103.
14. Nicholls, J. M., Poon, L. L., Lee, K. C., Ng, W. F., Lai, S. T., Leung, C. Y., Chu, C. M., Hui, P. K., Mak, K. L., Lim, W., *et al.* (2003) *Lancet* **361,** 1773–1778.
15. Peiris, J. S. M., Lai, S. T., Poon, L. L. M., Guan, Y., Yam, L. Y. C., Lim, W., Nicholls, J., Yee, W. K. S., Yan, W. W., Cheung, M. T., *et al.* (2003) *Lancet* **361,** 1767–1772.
16. Tse, G. M., To, K. F., Chan, P. K., Lo, A. W., Ng, K. C., Wu, A., Lee, N., Wong, H. K., Mac, S. M., Chan, K. F., *et al.* (2004) *J. Clin. Pathol.* **57,** 260–265.
17. To, K. F. & Lo, A. W. (2004) *J. Pathol.* **203,** 740–743.
18. Li, W., Moore, M. H., Vasilieva, N., Sui, J., Wong, S. K., Berne, M. A., Somasundaran, M., Sullivan, J. L., Luzuriaga, K., Greenough, T. C., *et al.* (2003) *Nature* **426,** 450–454.
19. Zhan, J., Chen, W., Li, C., Wu, W., Li .J., Jiang, S., Wang, J., Zeng, Z., Huang, Z. & Huang, H. (2003) *Clin. Med. J.* **116,** 1265–1266.
20. Leung, W. K., To, K. F., Chan, P. K., Chan, H. L., Wu, A. K., Lee, N., Yuen, K. Y. & Sung, J. J. (2003) *Gastroenterology* **125,** 1011–1017.
21. Rott, R., Orlich, M. & Blodorn, J. (1975) *Virology* **68,** 426–439.
22. Nagai, Y., Klenk, H. D. & Rott, R. (1976) *Virology* **72,** 494–508.
23. Ohuchi, M. & Homma, M. (1976) *J. Virol.* **18,** 1147–1150.
24. Tashiro, M., Yokogoshi, Y., Tomita, K., Seto, J. T., Rott, R. & Hido, H. (1992) *J. Virol.* **72,** 11–16.
25. Ng, M.-L., Tan, S.-H., See, E. E., Ooi, E. E. & Ling, A. E. (2003) *J. Gen. Virol.* **84,** 3291–3303.
26. Tashiro, M., Ciborowski, P., Klenk, H.-D., Pulverer, G. & Rott, R. (1987) *Nature (London)* **325,** 536–537.
27. Kishida, N., Sakoda, Y., Eto, M., Sunaga, Y. & Kida, H. (2004) *Arch. Virol.* **149,** 2095–2140.